Dissertationes Forestales 355

Toward an enhanced characterization of seedling stands using remote sensing

Mohammad Imangholiloo

Department of Forest Sciences
Faculty of Agriculture and Forestry
University of Helsinki

Academic dissertation

To be presented for public examination with the permission of the Faculty of Agriculture and Forestry of the University of Helsinki, in the Walter Auditorium of the EE-building, Agnes Sjöbergin katu 2, Helsinki on October 25th, 2024 at 12 o'clock noon.

Title of dissertation: Toward an enhanced characterization of seedling stands using remote sensing
Author: Mohammad Imangholiloo

Dissertationes Forestales 355
https://doi.org/10.14214/df.355

Thesis Supervisors:
Professor Markus Holopainen
Department of Forest Sciences, University of Helsinki, Finland

Research Professor Eija Honkavaara
Department of Remote Sensing and Photogrammetry, National Land Survey of Finland, Finland

Professor Mikko Vastaranta
School of Forest Sciences, University of Eastern Finland, Finland

Pre-examiners:
Associate Professor Hans Ole Ørka
Department of Forestry and Renewable Energy Section, Norwegian University of Life Sciences (NMBU), Norway

Associate Professor Kenneth Olofsson
Department of Forest Resource Management; Division of Forest Remote Sensing, Swedish University of Agricultural Sciences (SLU), Sweden

Opponent:
Research Professor Petteri Packalen
Bioeconomy and Environment Unit, Natural Resources Institute Finland (LUKE), Finland

ISSN 1795-7389 (online)
ISBN 978-951-651-800-1 (pdf)

Publishers:
Finnish Society of Forest Science
Faculty of Agriculture and Forestry of the University of Helsinki
School of Forest Sciences of the University of Eastern Finland

Editorial Office:
Finnish Society of Forest Science
Viikinkaari 6, FI-00790 Helsinki, Finland
http://www.dissertationesforestales.fi

Imangholiloo M. (2024). Toward an enhanced characterization of seedling stands using remote sensing. Dissertationes Forestales 355. 60 p. https://doi.org/10.14214/df.355

ABSTRACT

Seedling stands are areas in forest landscapes where young trees, typically from newly planted or naturally regenerated seedlings, grow. These stands are in the early stages of forest development and are crucial for the renewal and future growth of the forest. They represent a vital phase in the forest's lifecycle, for which careful management is often employed to ensure the successful establishment and growth of young crop trees.

To address the data-gathering requirements of forest management, seedling stands are typically assessed through field visits, a process that is considered time-consuming, expensive, and labor-intensive. As trees in the seedling stands are small and often densely stocked, they are difficult to assess in operational remote sensing-based forest inventories. However, recent developments in remote sensing, especially in laser scanning and the use of drones, could open new pathways to developing methods for the spatially explicit and timely inventorying of seedling stands; such methods could complement or even replace field visits.

The aim here was to develop and assess remote sensing methods of estimating the tree density, mean tree height, and species of seedling stands, which are the key characteristics supporting forest management. For this purpose, new remote sensing techniques–namely drone photogrammetric point clouds, hyper- and multi-spectral imagery (studies **I** and **IV**), and multi-spectral and single-photon airborne laser scanning (ALS; studies **II** and **III**) data–were investigated over seedling stands located in three study sites in the boreal forests of Finland. Performance of leaf-off and leaf-on hyper-spectral drone imagery and multi-spectral ALS data was explored in seedling stands in studies **I** and **II**. A canopy-thresholding method (C_{th}) was also optimized to minimize the interference of understory vegetation (study **II**), and the performance of single-photon ALS was examined in study **III**. In that study, an area-based approach (ABA) that included single-tree features and corrected the effect of edge trees ($ABA_{EdgeITD}$) was developed and compared to conventional ABA. In study **IV**, a new approach for feeding multispectral drone images to convolutional neural networks was proposed and validated for the classification of seedling tree species.

The findings of this thesis demonstrated that drone imagery yielded more accurate tree density estimates, while dense multispectral ALS data outperformed other tested methods of tree height estimation (both when using leaf-on data). The use of $ABA_{EdgeITD}$ improved the tree density and height estimates compared to conventional ABA, although it was less accurate than the individual tree-based methods used in studies **I** and **II**. Characterization of advanced seedling stands was more accurate than that of early-growth stage stands (mean height < 1.3 m), which remained challenging. Finally, the image pre-processing approach, together with the convolutional neural network, used in study **IV** improved the species classification accuracy of seedlings. This thesis shows that the remote sensing methods used can be applied in operational forest inventories to complement or replace field visits. These new technologies are valuable approaches to increasing the efficiency and sustainability of forest management.

Keywords: LiDAR, drone imagery, airborne laser scanning, regenerating stands, forest inventory, convolutional neural network

PREFACE

The journey of my PhD research began after the completion of my MSc thesis with Simosol Oy and a teaching assistant role in Remote Sensing 1 (spring 2017) at the University of Helsinki, which transitioned into a research assistantship at the Lab of Forest Resources Management and Geoinformatics at the University of Helsinki. It was during this time that Markus first discussed with me the challenges of extending remote sensing into seedling stands, sparking the idea that would become the foundation of my PhD research.

I would like to express my sincere gratitude to all those who have supported and guided me throughout my doctoral studies. This thesis would not have been possible without the invaluable contributions of numerous individuals who enlisting their names needs pages, and I am deeply indebted to each and every one of them.

First and foremost, I am grateful to my supervisors, Professors Markus Holopainen, Eija Honkavaara, and Mikko Vastaranta, for their unwavering support, guidance, and encouragement. Their expertise and mentorship have been instrumental in shaping the direction and content of this thesis. I am truly thankful for their patience, wisdom, and dedication to my academic and professional development.

I am also thankful to the members of my thesis committee, Professors Pasi Puttonen, Jari Hynynen, and Juha Hyyppä, for their invaluable feedback, insightful suggestions, and constructive criticism. Their collective expertise and diverse perspectives have significantly enriched the quality and depth of this work.

I am also thankful for the fruitful collaborations with my co-authors and data providers, as well as the individuals who contributed to the field work and collection of reference data for my studies. Their contributions have been essential to the development and completion of this thesis.

Verbal expression falls short in conveying the depth of gratitude I feel toward my parents and siblings for their unwavering support, encouragement, understanding, and patience during the ups and downs of my period of PhD research and studying abroad.

I would like to extend my heartfelt thanks to my colleagues and friends for their support, assistance, and encouragement throughout this journey. Their contributions have been invaluable to the successful completion of this thesis. Each one of them made an important contribution for this thesis to become at this stage. Special thanks to our daily fellow members of our lunch hour, Markus, Topi, Jiri, Ville, Einari, Otto, Mikko, Ville for brightening our moments, and providing opportunities for informal Finnish communications.

Finally, I am grateful for the research funding from the Doctoral Program in Sustainable Use of Renewable Natural Resources (AGFOREE) at the University of Helsinki, the Ministry of Agriculture and Forestry, and the Academy of Finland Flagship Forest-Human-Machine Interplay—Building Resilience, Redefining Value Networks and Enabling Meaningful Experiences (UNITE). Their financial support has enabled me to pursue my academic and research interests with dedication and focus.

In conclusion, I am truly grateful to all those who have contributed to the successful completion of this thesis. Their support and guidance have been invaluable, and I am deeply appreciative of their contributions to this work.

Helsinki, February 2024

Mohammad Imangholiloo

This tool aims to offer a comprehensive summary of the text in this PhD thesis by identifying the most commonly used keywords and displaying them in a tree shape. The tool was developed in-house using *WordCloud* Python module (http://amueller.github.io/word_cloud/)

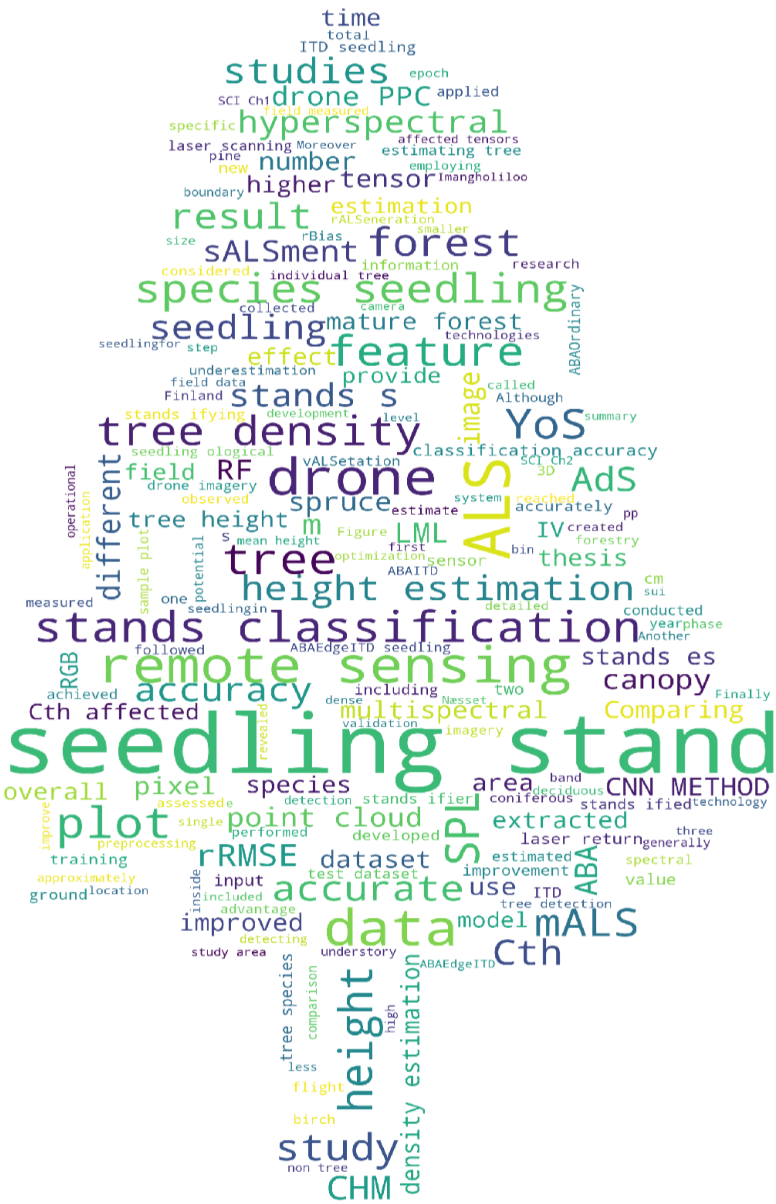

LIST OF ORIGINAL ARTICLES

This thesis is based on findings presented in the following articles, referred to by the Roman Numerals I–IV.

I Imangholiloo M, Saarinen N, Markelin L, Rosnell T, Näsi R, Hakala T, Honkavaara E, Holopainen M, Hyyppä J, Vastaranta M (2019) Characterizing Seedling Stands Using Leaf-Off and Leaf-On Photogrammetric Point Clouds and Hyperspectral Imagery Acquired from Unmanned Aerial Vehicle. Forests 10(5), article id 415. https://doi.org/10.3390/f10050415

II Imangholiloo M, Saarinen N, Holopainen M, Yu X, Hyyppä J, Vastaranta M (2020) Using Leaf-Off and Leaf-On Multispectral Airborne Laser Scanning Data to Characterize Seedling Stands. Remote Sens 12(20), article id 3328. https://doi.org/10.3390/rs12203328

III Imangholiloo M, Yrttimaa T, Mattsson T, Junttila S, Holopainen M, Saarinen N, Savolainen P, Hyyppä J, Vastaranta M (2022) Adding single tree features and correcting edge tree effects enhance the characterization of seedling stands with single-photon airborne laser scanning. ISPRS J. Photogramm. Remote Sens. 191: 129–142. https://doi.org/10.1016/j.isprsjprs.2022.07.005

IV Imangholiloo M, Luoma V, Holopainen M, Vastaranta M, Mäkeläinen A, Koivumäki N, Honkavaara E, Khoramshahi E (2023) A New Approach for Feeding Multispectral Imagery into Convolutional Neural Networks Improved Classification of Seedlings. Remote Sens 15(21), article id 5233. https://doi.org/10.3390/rs15215233

AUTHOR'S CONTRIBUTION

I) Imangholiloo designed the study together with his supervisors, conducted all the data analysis on procured the drone RGB, hyperspectral, and photogrammetric point cloud datasets, wrote the first draft of the manuscript, and revised it based on suggestions given by co-authors.

II) Imangholiloo designed the study together with his supervisors, developed the optimization method based on canopy height threshold (C_{th}) for minimizing the encounter of laser returns from understory, conducted all the data analyses of multispectral airborne laser scanning datasets, wrote the first draft of the manuscript, and revised it based on suggestions given by co-authors.

III) Imangholiloo designed the study together with his supervisors, developed the method of including features extracted from individual trees and correcting the effect of edge trees ($ABA_{EdgeITD}$), conducted all the data analyses of conventional linear-mode and single-photon laser scanning datasets, wrote the first draft of the manuscript, and revised it based on suggestions given by co-authors.

IV) Imangholiloo designed the study together with his supervisors, planned the field data collection procedure, proposed and developed the new method for image preprocessing based on C_{th} to be implemented before feeding input tensors into the convolutional neural networks (CNN), conducted all the data analyses, wrote the first draft of the manuscript, and revised it based on suggestions given by co-authors.

TABLE OF CONTENTS

ABBREVIATIONS

3D	Three dimensional
ABA	Area-based approach
ABA_{Edge}	Area-based approach improved by correcting edge tree effects
$ABA_{EdgeITD}$	Area-based approach improved by correcting edge trees and adding ITD
ABA_{ITD}	Area-based approach improved by adding ITD features
$ABA_{Ordinary}$	Area-based approach ordinary or conventional (is the same as ABA)
AdS	Advanced seedling stand
AI	Artificial intelligence
ALS	Airborne laser scanning
CHM	Canopy height model
CNN	Convolutional neural network
C_{th}	Canopy threshold height
dbh	Diameter at breast height
DLS	Downwelling light sensor
DTM	Digital terrain model
GCP	Ground control point
GNSS	Global navigation satellite system
ITD	Individual tree detection
LiDAR	Light detection and ranging (laser scanning)
LML	Linear-mode LiDAR
LOOCV	Leave-one-out cross validation
mALS	Multispectral airborne laser scanning
MCI	Multi-channel intensity
ML	Machine learning
NDVI	Normalized difference vegetation index
NFI	National forest inventory
NIR	Near-infrared
OA	Overall accuracy
OLS	Ordinary least square (regression)
pp	Percentage point
PPC	Photogrammetric point clouds
PRAS	Remotely piloted aircraft systems
RF	Random forest
RGB	Red-green-blue
RMSE	Root mean square error
rRMSE	Relative root mean square error
RTK	Real-time kinematic positioning
SCI	Single-channel intensity
SPL	Single-photon LiDAR
TPH	Trees per hectare
UAS	Uncrewed aerial system
UAV	Uncrewed aerial vehicle
VI	Vegetation index
YoS	Young seedling stand

1 INTRODUCTION

1.1 Ecology and management of seedling stands

Seedling stands are essential for the early growth of young trees in forest ecosystems, and their careful management is crucial for sustainable forest growth, future wood supply security, and ecosystem health. Seedling stands are typically known as homogeneous forest stands in the early stages of development, with the mean height of crop species being <8–10 m (Næsset and Bjerknes 2001; Næsset et al. 2004; Nilsson et al. 2010; Bartels et al. 2016). They are also referred to as regenerating or young forest stands. In Finland, seedling stands are classified as young seedling stands (YoS), with a mean tree height of <1.3 m, and advanced seedling stands (AdS), with a mean tree height of <7 or <9 m in coniferous and deciduous stands, respectively (Tapio 2006). These stands make up a significant portion (17%) of the Finnish forest land available for wood supply (Korhonen et al. 2021). The growth stage of seedlings is crucial in even-aged forestry, and appropriate silvicultural operations are necessary for their successful establishment and growth. The increasing number of Finnish forest stands younger than 20 years old (Kuuluvainen and Gauthier 2018) highlights the importance of managing seedling stands to ensure the development of mature stands for wood and other forest products.

The primary goal of forest silviculture in seedling stands is to establish productive forests following clearcutting (Rantala 2011), which has been a central principle of forest treatments in Finland for over a hundred years (Rantala 2011). This is to ensure sustainable wood supply for the future (Rantala 2011; Huuskonen et al. 2020). In the years following clearcutting, new seedlings naturally emerge from seeds of retention trees or are manually planted (Mielikäinen and Hynynen 2003). In Finland, it is common practice to plant approximately three to four new seedlings for every harvested mature tree (MetsäGroup 2020), while in Sweden, at least two seedlings are typically planted (Berglund 2021). Manual planting becomes necessary in areas where the natural regeneration of crop species has not been successful. According to the Finnish Forest Act (1996/1039), it is mandatory to establish a financially viable seedling stand within 10–25 years of clearcutting, ensuring sufficient seedling density, with a mean height of >0.5 m and no immediate treatment of other vegetation. Furthermore, deciduous seedlings, particularly birch (Hynynen et al. 2010), often outgrow coniferous seedlings in the early growth stages of Nordic forests (Kaila et al. 2006; Uotila 2017). Therefore, it is crucial to release coniferous seedlings from the dominance of unwanted deciduous seedlings and understory vegetation (Uotila 2017; Äijälä et al. 2019; De Lombaerde et al. 2021; Dumas et al. 2022).

During the early stages of forest stand development, two primary silvicultural operations are commonly implemented: tending, which involves the removal of competing understory and non-crop trees to favor the growth of desired crop trees, and thinning, which entails the selective removal of unwanted trees that compete with the crop trees. Tending activities are typically conducted within 5–10 years after planting, while thinning operations are initiated when the trees have reached a height of 1–5 m, a stage typically attained within approximately 10 years of initial planting. These silvicultural operations play a critical role in ensuring the successful establishment, survival, and optimal growth of the desired crop species in the forest stand.

The regeneration of seedling stands and the implementation of silvicultural tending are recognized as the two most costly forest operations, with estimated expenses of 940 and 423 €/ha, respectively (Äijälä et al. 2019; Kellomäki et al. 2021, 2023).

Despite the substantial financial costs associated with these operations, they are widely acknowledged as essential long-term investments in forest management (Äijälä et al. 2019). Moreover, Huuskonen et al. (2020) have underscored that a significant increase in stumpage revenues, amounting to €1.7 billion over the subsequent 100-year period, could be realized through a corresponding rise of €560 million in expenditures for more proactive seedling management in Finnish forests. These seedling operations are instrumental in ensuring the appropriate stocking of crop species and the establishment and growth of trees for future wood supply. Research has indicated that these operations contribute to the increased profitability of forest stands as they reach mature stages (Huuskonen and Hynynen 2006; Uotila and Saksa 2014; Ara et al. 2022). Consequently, there is a need to apply these operations in a highly cost-effective manner to enhance the survival, establishment, and growth of crop seedlings (Nilsson et al. 2010). Figure 1 shows a typical seedling stand.

1.2 Collecting the information required for management of seedling stands

Tree density, height, and species are the most crucial forest attributes to consider in the management of seedling stands, alongside survival, growth, species composition, and stocking (Næsset and Bjerknes 2001; Næsset et al. 2004; Vepakomma et al. 2023). Traditionally, this information is gathered through field visits, which are considered to be labor-intensive, less spatially explicit, and costly. In the context of national forest inventories (NFIs), forest plots are systematically sampled to measure the number of conifer and broadleaf trees per hectare, their heights, as well as additional data such as the tree species, diameter at breast height (dbh), tree stem quality, and canopy layer, particularly in mature forests. The field plots are typically circular and of varying radii based on tree dbh, with specific radii or relascope factors used for different dbh ranges (Korhonen et al. 2021). In seedling stands, tree species and story are used to define tree strata. Specific attributes such as mean height, mean diameter, age, basal area, and number of stems, together with seedling age, seedling damage, regeneration type (natural or cultivated), and other categorical stand attributes, are then assessed (Korhonen et al. 2021; Rana et al. 2023).

Figure 1. An oblique image captured with a drone showing seedling stands on both sides of the road, with mature stands on the right and upper sides of the image.

1.3 Remote sensing techniques for characterizing seedling stands

Remote sensing (RS) technologies and methods have undergone rapid advancement in recent decades, resulting in enhanced spatial explicitness, accessibility, cost-effectiveness, and the capacity to gather data across extensive areas within a relatively short time frame. Consequently, RS has the potential to provide information of superior spatial accuracy and in a more timely manner, thereby supporting silvicultural decision-making processes pertaining to the management of treatments in seedling stands. Consequently, there is an impetus to develop and swiftly implement novel methods that can effectively cater to the evolving requirements of foresters in the face of today's changing world under various climate threats.

1.3.1 Satellite images and aerial photographs

Different RS techniques, including the generation of air- or space-borne optical and radar data, have been employed in the monitoring of seedling stands. For instance, synthetic aperture radar (SAR) is an active RS technique that measures the distances between objects and sensors indirectly using microwaves. SAR can be utilized from space or sky to collect valuable data for mapping and monitoring seedling stands. Akbari et al. (2021) utilized open-access SAR data from the Sentinel-1 satellite in combination with optical images from the Sentinel-2 satellite in a multi-temporal manner to detect and characterize seedling stands in Norway. Mitri and Gitas (2013) used a combination of high-resolution satellite imagery (QuickBird) and hyperspectral satellite data (EO-1 Hyperion) to map forest regeneration and vegetation recovery after fire. Additionally, Wunderle et al. (2007) used SPOT-5 satellite imagery to assess regenerating boreal forests, while Häme (1984) interpreted coniferous and deciduous seedling stands using Landsat imagery.

Aerial imagery has also been employed in the assessment of seedling stands. For example, Kirby (1980) used aerial photogrammetry systems with manual interpretation to assess the regeneration of coniferous seedlings taller than 30 cm in Alberta, Canada, and Hall and Aldred (1992) used them to assess tree density and stocking in forest regeneration areas on a large scale. Smith et al. (1986) utilized high resolution aerial photography to image and identify pine seedlings after the first growing season. Additionally, Ball and Kolabinski (1979) and Haddow et al. (2000) utilized color aerial imagery to assess softwood regeneration, and to detect conifer seedlings and assess their competition, respectively. Furthermore, Pouliot et al. (2005, 2006) conducted an automated assessment of tree detection and the mapping of competition between trees and shrubs via aerial imagery. Although each of the abovementioned methods has its own merits, high resolution aerial imagery using drones and computer-assisted image interpretation methods have become particularly common, gradually replacing manual methods of tree detection.

1.3.2 Airborne laser scanning technology

Airborne laser scanning (ALS) has been a transformative RS technique for the monitoring and assessment of forest and vegetation canopies. It operates by emitting and receiving high-energy, specific-wavelength laser beams to measure distances based on the time of light travel (Wehr and Lohr 1999; Lefsky et al. 1999, 2002). The distance is measured by time-of-flight of the light in a 3D space (Bachman 1979). This method provides highly accurate and detailed 3D information (Wehr and Lohr 1999; Montaghi et al. 2013), particularly for forest structures at various scales, and is especially effective in capturing detailed 3D data related to tree height (Beland et al. 2019). Usually mounted on aircraft, it can quickly scan large areas at the scale of thousands of square kilometers (Wulder et al. 2012), making it an efficient tool for broad-scale monitoring. It has revolutionized forest RS by providing accurate and detailed 3D data of forests and vegetation canopies, which were previously difficult to obtain.

One of the key advantages of ALS is its ability to operate independently of sunlight, as it relies on its own laser beams. However, its effectiveness can be hindered by cloud cover, dense fog, or dust, depending on the wavelength of the laser beams. Despite this limitation, ALS has been used for large-scale operational data collection, such as national-level ALS data from Finland and other Nordic countries. While national ALS data from Finland provide valuable information about mature forests, the data obtained from seedling stands may be less detailed. This necessitates the acquisition of higher-quality ALS data, which can be obtained via helicopter or drone.

The development of ALS sensors to enhance efficiency and accuracy has been ongoing. For instance, single-photon laser (SPL) scanning has enabled the collection of highly detailed data over large areas by utilizing advanced technology that relies on a 10×10 practical laser beam (called beamlet) and high sensitivity for recording laser returns (Degnan 2016; Beland et al. 2019). It produces six million pulses per second using very short laser pulses in the green wavelength region of 532 nm (Leica 2021). Compared to conventional laser scanning systems, it has been found to detect backscattered laser returns more accurately, rapidly, and efficiently (Swatantran et al. 2016). Additionally, multispectral ALS (mALS) sensors have been developed to scan using multiple beams at different wavelengths, enabling better and more detailed spectral characterization and higher point density. These advancements have made ALS a potentially single-sensor solution for remote sensing applications (Yu et al. 2017). Terrestrial laser scanning is a type of laser scanning that involves mounting the sensor on ground tripods, providing the ability to capture highly detailed 3D data of the surrounding environment. However, it has been underutilized in the assessment of seedling stands due to the high occlusion effect caused by dense tree density.

1.3.3 Drone imagery technology

The use of drones, also known as uncrewed aerial vehicles (UAV), uncrewed aerial systems (UAS), or remotely piloted aircraft systems (RPAS), has become increasingly popular in forestry research and industry. Drones equipped with various sensors, including optical (RGB, NIR, multispectral, or hyperspectral) or active (LiDAR or SAR) sensors, have been utilized for collecting high-resolution imagery to estimate essential forest inventory variables, with accuracies close to those achieved through field visits (Tuominen et al. 2015; Zahawi et al. 2015; Torresan et al. 2017; Goodbody et al. 2019; Puliti et al. 2019). This thesis focuses on drone optical imagery.

Drones offer a cost-effective and repeatable method of collecting very high spatial resolution data for smaller areas (Carr and Slyder 2018; Albuquerque et al. 2021; Lopatin and Poikonen 2023; Fassnacht et al. 2024), providing benefits for the detection and characterization of small trees in young or recovering forest stands (Zahawi et al. 2015; Thiel and Schmullius 2017; Puliti et al. 2019). This includes the collection of data on seedling density, height, species, distribution, and health, which can aid foresters in applying the necessary seedling treatments at the right time and place. Moreover, Goodbody et al. (2018) used aerial photogrammetry and drone-PPC to assess the conditions of seedling stands, while Korpela et al. (2008) demonstrated successful assessment of vegetation in seedling stands using a combination of aerial photography and ALS.

However, drones have limitations in covering large spatial areas, operating at large scales due to safety regulations and technological constraints, and facing variability in data quality depending on weather conditions. Additionally, there are high workload and administrative costs associated with large-scale drone survey applications, such as travel to survey sites (Puliti et al. 2017; Fassnacht et al. 2024).

Drones capture RGB, multispectral, and/or hyperspectral data, which are processed to provide orthomosaics using photogrammetric techniques. RGB images are commonly used due to their low cost and comparable results to ALS data (Fassnacht et al. 2024). The RGB images can also be used to create 3D photogrammetric point clouds (PPCs) using a photogrammetric method named "structure from motion," the image processing technique of generating 3D point clouds using several 2D images with different view angles to the object (Snavely et al. 2008; Guimarães et al. 2020). These PPCs can be very dense but, unlike ALS, cannot penetrate to the interior or bottom of the canopy.

From an imagery perspective, drone images can be RGB, multispectral (often RGB with RedEdge, NIR, and SWIR spectral bands), or hyperspectral. Spectral reflectance bands of consumer RGB cameras are optimized for human eyes and not for remote sensing, while multispectral cameras, with 5–10 optimized bands, and hyperspectral cameras, typically with hundreds of narrow bands, provide precise spectral data (Aasen et al. 2018).

Overall, the use of drones in forestry has shown great potential for improving forest management and conservation efforts. Drones can complement or replace field visits for seedling stands and can be a feasible alternative where frequent data collection is needed or where ALS data are not available (Thiel and Schmullius 2017).

1.4 Methods of tree density and height estimation in seedling stands

1.4.1 Area-based approach (ABA)

The area-based approach (ABA) utilizes statistical relationships between predictor variables obtained from ALS data (such as height percentile) and target variables from field-measured plots to predict forest inventory parameters such as volume and basal area (Næsset 2002; White et al. 2013a). It involves acquiring ALS data for the area of interest, gathering field measurements, and developing predictive parametric (e.g., regression) or non-parametric models, followed by applying these models to produce wall-to-wall estimates and maps of particular forest inventory parameters (White et al. 2013a). ABA is not reliant on subjective stand boundaries and can forecast forest attributes with superior or comparable accuracy to conventional field inventories (Næsset 2004; White et al. 2013a). Additionally, integrating optical data with ALS data can enhance the estimation of forest characteristics at the species-specific level (Packalén and Maltamo 2007). ABA is widely accepted and operational in forest inventories (White et al. 2013a; Næsset 2014), particularly in Nordic countries (Næsset 2004; Næsset 2014; Nilsson et al. 2017; Maltamo et al. 2021), and is a low-cost method (Eid et al. 2004; Næsset 2004).

Efforts have been made to enhance the performance of conventional or "ordinary" ABA methods ($ABA_{Ordinary}$) of characterizing different forest stands. These efforts can be categorized into two approaches:

1) *Adding individual tree features into ABA (ABA_{ITD})*: This approach combines individual tree detection (ITD, explained in Section 1.4.2) with $ABA_{Ordinary}$ methods by averaging the features extracted from ITD segments within plots and using them for statistical modeling of forest attributes. This approach was initially introduced by Hyyppä et al. (2012), then further investigated and verified in other studies in mature forests (Breidenbach et al. 2012; Vastaranta et al. 2012; Shinzato et al. 2017; Parkitna et al. 2021; Kelley et al. 2022).

2) *Correcting the effect of edge or border trees in plot boundaries (ABA_{Edge})*: This approach involves adjusting the boundary of forest plots based on segmented edge treetops to improve consistency between ALS-derived features and plot-level field measurements. This approach was first introduced by Packalen et al. (2015), then evaluated and corroborated in other studies in mature forests (Pascual 2019; Knapp et al. 2021; Kotivuori et al. 2021).

1.4.2 Individual tree detection (ITD) methods

The ITD methods detect individual treetops, fit a crown boundary for each tree to be used for extracting different features from the point clouds, or image pixels located inside each tree segment. The ITD methods use a rasterized canopy height model (CHM; representing the height of each pixel from the ground) or point cloud directly (e.g., Hyyppä and Inkinen 1999; Wang et al. 2016). The typical components of tree detection are the different spatial spacing between individual trees, different inner or outer structure of trees, and geometric- and intensity-related properties of ALS point clouds (Parkan 2019). The CHM-based ITD methods typically find treetops using local maxima, then segment the crown boundary for individual or groups of trees using a segmentation algorithm such as marker-controlled watershed segmentation, which finds catchment basins on the CHM considered to be flooded topographic reliefs (Kornilov et al. 2022). Point cloud-based ITD methods often voxelize the point clouds and cluster them to distinguish the individual trees (Wang et al. 2016). The estimated forest attributes from these different ITD methods can be assessed at the tree, plot, or stand level (Vastaranta et al. 2011). Given the need for high-density point cloud data to detect individual seedlings, earlier applications of the ITD method were often elusive in characterizing seedling stands.

1.5 Remote sensing methods of classifying species of seedlings

1.5.1 Machine learning methods

Spectral data from images and the intensity of mALS data are commonly utilized to classify species in remote sensing-based forest inventories. Machine learning (ML) methods can be categorized into supervised, semi-supervised, and unsupervised methods based on the availability of target variables (e.g., species class) and training data. This thesis focuses on the use of supervised methods, which utilize artificial intelligence (AI) to interpret data and achieve specific goals and tasks (Kaplan and Haenlein 2019).

A popular ML method used for classifying different objects, including tree species classes, is the random forest (RF) algorithm. RF is an ensemble method that creates uncorrelated and independent decision trees to predict the target variable (Breiman 2001).

The most-voted prediction among the decision trees is used as the final predicted class (Breiman 2001) or the class with the highest average of prediction probability among classes in the implementation of RF using scikit-learn software (Pedregosa et al. 2011). It is a supervised learning method that trains a predictive model on input features and the target label to predict the target variable of unseen test data. It is known for its speed, ease of use, robustness to noise, high dimensionality, and multicollinearity of data, as well as its insensitivity to overfitting (Breiman 2001; Gislason et al. 2006; Cutler et al. 2007; Fawagreh et al. 2014; Belgiu and Drăgu 2016). The training phase often employs a cross-validation mechanism with out-of-bag sampling to reduce the risk of overfitting and improve model performance and generalization ability (Berrar 2019; Kee et al. 2023).

RF, along with other ML methods, has been extensively utilized in forestry applications, such as for classifying tree species (Immitzer et al. 2012; Dalponte et al. 2013; Fassnacht et al. 2014; Shang and Chisholm 2014; Ma et al. 2021; Quan et al. 2023), mapping forest health conditions (Wang et al. 2015; Fraser and Congalton 2021; Huo et al. 2021; Junttila et al. 2022), and predicting the regeneration probability of coniferous seedlings (Zhao et al. 2023). For instance, Zhao et al. (2023) reported that among all the methods they tested, RF had the highest accuracy in predicting the regeneration probability of coniferous seedlings.

1.5.2 Convolutional neural network (CNN) methods

Convolutional neural networks (CNNs) are another type of AI that is particularly effective for image classification tasks. CNNs consist of interconnected processing units organized in convolutional layers of intercorrelated nodes, where weights and biases are applied to input images to generate new feature maps (Ma et al. 2019; Kattenborn et al. 2021). To put it simply, the input data undergo convolutional computations in each convolutional layer when they pass forward and become ready for a decision (species class) made in the last layer using the values produced in each layer (Kim 2017; Litjens et al. 2017; Ma et al. 2019; Alzubaidi et al. 2021). Unlike traditional ML methods, CNNs can automatically create relevant features directly from input images (Sewak et al. 2018), eliminating the need for pre-defined manually created features and preprocessing (Li et al. 2017; Gao et al. 2018; Mäyrä et al. 2021).

CNNs have gained popularity in RS-based image classification (Kattenborn et al. 2021), especially in the context of tree species classification in mature forests and other forestry applications. They have been successfully applied in the classification of tree species using various image inputs, including RGB and multi- and hyper-spectral images collected from drones, and air- and space-borne remote sensing platforms (e.g., Fricker et al. 2019; Natesan et al. 2020; Nezami et al. 2020; Pleşoianu et al. 2020; Onishi and Ise 2021; Yan et al. 2021). Additionally, CNNs have been used for tree health mapping (Minařík et al. 2021; Kanerva et al. 2022; Safonova et al. 2022; Turkulainen et al. 2023) and have demonstrated superior performance over other ML methods, such as RF, in species classification in mature forests (Mäyrä et al. 2021; Yan et al. 2021) and urban or suburban areas (Li et al. 2021; Guo et al. 2022), yet largely remain unstudied for the classification of seedling stands.

1.6 Remote sensing methods of estimating tree height in seedlings

The estimation of tree height through RS involves extracting the maximum height point (H_{max}) from normalized point clouds obtained from ALS or drone-PPC data within tree canopy segments using the ITD method or modeling in ABA methods (Wang et al. 2019). The same approach can also be applied to estimate the height of seedlings. However, the accurate estimation of tree height in forests is challenging due to factors such as dense canopy cover, steep terrain (Gatziolis et al. 2010), a tall and dense understory (Haugerud et al. 2003; Hyyppä et al. 2008; White et al. 2013a), as well as the point density of the ALS data used (Hyyppä et al. 2008), as low-density ALS data are generally expected to hit tree "shoulders" rather than treetops (Nelson et al. 1988).

These challenges hinder the generation of accurate digital terrain models (DTM) for height normalization, leading to difficulties in tree height estimation. This is particularly challenging in seedling stands because the same error in estimating the height of a small tree results in a proportionally larger error in seedling height compared to the error in tall trees. Additionally, seedlings are more vulnerable to point density issues as their sharp treetops lower the chance of ALS hitting the treetops, thus causing larger underestimates, as observed in the studies conducted in this thesis.

1.7 State of the art and objectives

The utilization of drone and ALS data in seedling stands had been relatively limited prior to the commencement of this thesis, with little prior exploration in both research and operational applications. While drone imagery has demonstrated promising results in the monitoring of mature forests, the research in this thesis has opened new avenues for understanding the potential of drones in seedling stands and has unlocked their full potential for use. Except for several studies that applied drone multispectral or RGB data in seedling stands (e.g., Vepakomma et al. 2015; Feduck et al. 2018; Goodbody et al. 2018; Puliti et al. 2019), before the realization of this thesis project, seedling stands had not been studied using hyperspectral drone imagery (study **I**), and the comparison of the suitable acquisition times for leaf-off and leaf-on data and investigation of methods in YoS and AdS had not been thoroughly explored prior to study **I**. Furthermore, study **I** was the first to utilize ITD in seedlings, in contrast to the use of ABA in inputs of ALS and PPC data by Puliti et al. (2019). The focus of study **I** was on assessing overall and spruce-specific tree density and height in seedling stands, given the greater care (e.g., tending and thinning to free them from naturally grown birches) required by spruces as the main crop species, compared to pine seedlings.

In addition to the novelty of using mALS in seedling stands in study **II**, other innovations included the optimization of the canopy height threshold (C_{th}) method to minimize the encounter of laser returns from below the canopy in seedling stands, as well as the comparison of leaf-off and leaf-on conditions in YoS and AdS plots. Although the $ABA_{Ordinary}$ method was widely used in operational forestry, it had challenges inventorying seedling stands using nationwide low-density ALS data, remaining less operational and less developed for seedling stands. Therefore, study **III** pioneered the exploration of SPL in seedling stands and the development of the $ABA_{EdgeITD}$ method, while also comparing YoS and AdS.

While some previous studies had used CNN to detect seedlings (e.g., Chadwick et al. 2020; Pearse et al. 2020; Jayathunga et al. 2023; Lopatin and Poikonen 2023), they did not focus on addressing classification issues in seedling stands. Therefore, study **IV** focused on the use of CNN for classifying seedling species and developed a new C_{th}-based image preprocessing method to be applied before feeding image tensors to the CNN classifiers. This is particularly important as the capability of CNNs to classify species in seedling stands–where classification is challenging due to factors such as varying canopy sizes, low foliage cover percent, and mixed reflectance from neighboring trees or understory vegetation–has not been extensively examined. Study **IV** also compared the results with RF as a benchmark of ML methods. Overall, this thesis has addressed some parts of the knowledge gap in this area.

The overarching aim of this thesis is to enhance the characterization of seedling stands using emerging RS techniques, with a specific focus on improving tree density estimation, mean tree height estimation, and species classification at either the tree or plot level. These are key forest characteristics that need to be considered in silvicultural operations to ensure the sustainability of seedling stands and the quality of the future forests and wood supply. The main objectives of each study are to:

1. Investigate the potential of drone-PPC and hyperspectral data to estimate the tree density and height of seedling stands in both leaf-off and leaf-on conditions (study **I**)
2. Minimize the impact of the understory by optimizing the C_{th} method to enhance estimation of the tree density, height, and species classification of seedling stands using mALS data in leaf-off and leaf-on conditions (study **II**)
3. Enhance the $ABA_{Ordinary}$ method by developing the $ABA_{EdgeITD}$ method to improve the tree density and height estimation of seedling stands tested using SPL and LML ALS data (study **III**)
4. Improve the species classification accuracy of seedlings by developing a preprocessing step in CNN on multispectral drone imagery (study **IV**)

2 MATERIALS AND METHODS

2.1 Study areas

The study areas consisted of different seedling stands that represented typical southern boreal seedling stands in Evo (61.20°N, 25.08°E; studies **I**, **II**, and **IV**) and Akaa (61.25°N, 23.24°E; study **III**), Finland.

The Evo study area covered approximately 2,000 hectares of forested land, with elevations ranging from 125 to 185 m above sea level. The dominant tree species in Evo were Scots pine (*Pinus sylvestris* L.) and Norway spruce (*Picea abies* (L.) H. Karst.), with deciduous species accounting for about one-fifth of the total stem volume. The primary deciduous tree species in Evo were silver birch (*Betula pendula* Roth) and white birch (*Betula pubescens* Ehrh.), and the site type of the area was classified as mesic heath forest.

The Akaa study area covered approximately 102,000 hectares of forested land, with elevations ranging from 75 to 150 m. Similarly to Evo, Scots pine and Norway spruce were the dominant species in Akaa, and the area was also characterized as a typical managed boreal forest.

The study areas are visually represented in Figure 2, providing a geographical overview of the Evo and Akaa locations.

2.2 Field data collection

The study sites for both study **I** and study **II** were selected based on existing forest resources information, with a focus on stands with a tree density of more than 2,400 trees per hectare (TPH). Field plots were established at different tree densities through thinning, with circular plot areas of 5 and 10 m considered for young seedling (YoS) and advanced seedling (AdS) stands, respectively. Thinning was carried out to achieve target tree densities ranging from approximately 1,200 to 2,000 TPH in YoS plots and 600 to 2,400 TPH in AdS plots. The establishment of sample plots, thinning, and recording of plot locations using the Trimble GeoXT Global Navigation Satellite System (GNSS) device were conducted from April to May 2016, followed by the measurement of plot-level forest inventory attributes in June 2016.

In this field measurement, the dbh and species of seedlings taller than 1.3 m were recorded in the AdS plots. Additionally, the height of every third seedling of each species and the height of the tallest seedling in each plot were measured. For the remaining seedlings in each plot, their heights were estimated using Näslund's height curve (Näslund 1936) and the sampled seedling height measurements. In the YoS plots, the diameter at ground height of the seedlings was measured, as the seedlings were generally shorter than 1.3 m.

The plot-level tree density was calculated by dividing the number of observed seedlings of each species by the area of each plot, converted to hectares. The plot-level mean height of the seedlings was calculated by taking the arithmetic average of the seedling heights in single-species plots, and a weighted average of the mean height of species and their numbers in mixed-species plots. It is important to note that three plots (G1, G2, and G8) from the AdS were not included in study **II** because they were not thinned before the collection of leaf-off data on 1 May 2016. Table 1 shows the tree density and height variables in sample plots used in studies **I** and **II**. The remaining seedlings in the YoS were all spruce, while the AdS had an admixture of birch, accounting for less than 51% and 34.3% in studies **I** and **II**, respectively.

In study **III**, 85 circular plots were established as part of the operational forest inventory site of the Finnish Forest Center. The location of these plots was pre-defined using a systematic stratified sampling method to ensure representation of the structural variation of seedling stands in the study area. Field measurements were performed inside single 9-m or 5.64-m radius circular plots or four sub-plots with 2.82-m radii inside the 9-m radius circular plot (according to the growth stage and silvicultural management applied to the seedling stands) to ease the burden of field measurements. A total of 89 sample plots were measured, with the field crew recording the location of the plot center using GNSS and measuring the dbh and species of every tally tree within the plots. Additionally, the height of one tally tree per species and per height stratum were measured to be used for modeling the height of other trees using a mixed-effect model, which fits height-dbh curves for each species, proposed by Eerikäinen (2009).

In study **IV**, 14 seedling stands representing variations in tree density and species classes were selected, and stratified sampling was used to pre-define the sample locations and their numbers in each stand. The sample plots were positioned along the longest intersecting line drawn through each stand, with the field crew using a magnetic compass and measuring tape to determine the direction of intersecting lines and the location of the plot center. A Real-Time-Kinematic (RTK) GNSS device was used to record the location of the plot center, and the height, species, and location of all trees above 1 m in height were recorded. Depending on the height of the tree, either a measurement stick or an electrical clinometer (Vertex IV, Haglöfs Sweden) was used for measuring tree height. In the early development stages of mainly deciduous species, seedlings typically grow in thickets. The field crew were instructed to record one location for these thickets and report the number of unique seedlings taller than 1 m per species class in this location. A total of 5,417 seedlings inside 75 sample plots of 10×10 m were measured.

To ensure clarity, the forest inventorying in studies **I**–**III** was conducted at the plot level, while study **IV** focused on individual-tree level inventorying. For more in-depth information on the field data collection and forest inventorying methods employed in each study, please read the individual study descriptions. Table 1 offers a comprehensive summary of the data utilized in studies **I**–**IV**, and Figure 2 visually depicts the study areas.

Table 1. A summary of tree density and height measured from plots used in studies **I–IV**.

Study	Collection time	Data level	Measured attribute	Growth stage (number of observations)	Mean of tree density (range)	Mean of tree height (range)	Mean of tree density and height of	
							Spruce	Birch
I	June 2016	Plot level	Tree height, species, density	YoS (n = 5)	1591.6 (1194–1989)	1.1 (0.7–1.9)	1591.6, 1.1	0.0, NA
				AdS (n = 10)	1508.9 (605–2388)	3.3 (1.6–4.5)	1206.5, 3.0	432.0, 4.2
				All (n = 15)	1536.5 (605–2388)	2.5 (0.7–4.5)	1334.9, 2.3	432.0, 4.2
II	June 2016	Plot level	Tree height, species, density	YoS (n = 5)	1591.6 (1194–1989)	1.1 (0.7–1.9)	1591.6, 1.1	0.0, NA
				AdS (n = 7*)	1587.1 (796–2228)	3.2 (1.6–4.5)	1364.3, 3.0	390.0, 4.3
				All (n = 12)	1589.0 (796–2228)	2.3 (0.7–4.5)	1459.0, 2.2	390.0, 4.3
III	Summer 2017	Plot level	Tree height, species, density	YoS (n = 9)	6588.9 (1900–13700)	1.2 (0.8–1.3)	-	-
				AdS (n = 80)	3974.1 (1001–14200)	4.0 (1.4–7.8)	-	-
				All (n = 89)	4238.5 (1001–14200)	3.7 (0.8–7.8)	-	-
IV	September 2020	Tree level	Tree species, height	5417 seedlings tree-mapped in 75 sample plots of 10×10 m, included pine (13.6%), spruce (28.7%), birch (48.4%), and other species (9.3%)				

*****three plots were excluded from study **II**, because the plots were not thinned in preparation for remote sensing data collection for study **II** on 1 May 2016.

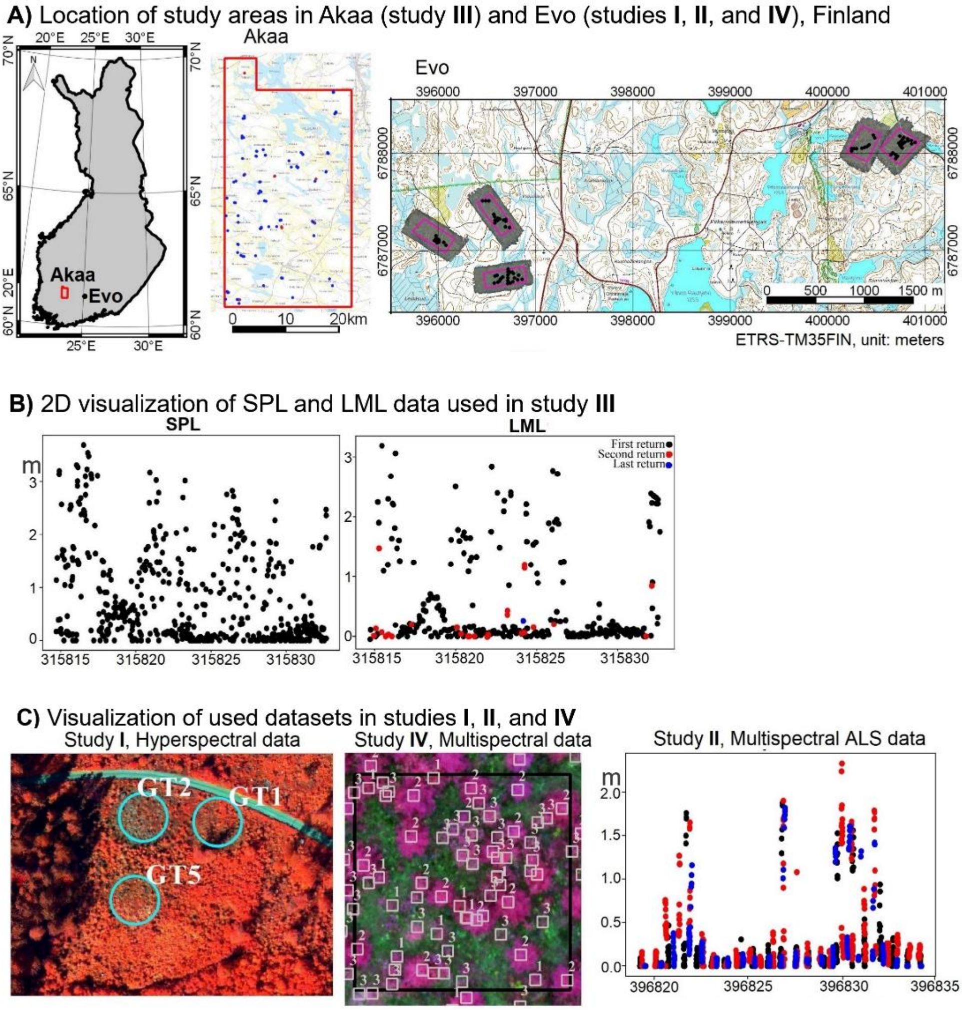

Figure 2. A) Map of the study areas used in this thesis, along with illustrations of small subsets of the data from each study. Studies **I**, **II**, and **IV** were performed in the Evo and study **III** in the Akaa study area in Finland. **B)** 2D visualization of single-photon and linear-mode laser scanning (SPL and LML) data visualized by laser return numbers. **C)** Visualization of hyperspectral and multispectral drone data (studies I and **IV**) in plot and tree level together with 2D visualization of multispectral ALS data (study **II**) colored by scanner channels 1550, 1064, and 532 nm in black, red, and blue, respectively.

2.3 Remote sensing data collection

The RS data used in this thesis included different optical (passive) imaging (hyperspectral, multispectral, and RGB) mounted on drones and different active ALS mounted on helicopters or other aircraft. Table 2 provides a summary of the data and Figure 2 visualizes parts of the data. However, the detailed technical specifications of the used data can be found in the published research articles of each study.

Table 2. Summary of used remote sensing data with other relevant information used in the different studies in this thesis.

Study	Platform	Sensor	Data type	Resolution	Acquisition time	Flight height
I	Drone	Fabry–Pérot interferometer (FPI)	Hyperspectral (36 spectral bands)	10 cm	9 and 11 May (Leaf-off) and 29 June (leaf-on) in 2016	100 m
		Samsung NX300	RGB	2.5 cm		
II	ALS	Optech Titan mALS scanner	Multispectral ALS (Channels in 532, 1064, and 1550 nm)	60.1 and 57.2 points/m^2 (leaf-off and leaf-on)	1 May (leaf-off) and 12–14 June (leaf-on) 2016	500 m
III	ALS	Leica (SPL100)	ALS in 532 nm	19.0 points/m^2	31 May 2018	3750 m
		Riegl VQ-1560i (LML)	ALS in 1064 nm (dual)	12.5 points/m^2	21–23 May 2018	1450 m
IV	Drone	MicaSense MX Red-Edge	Multispectral (RGB, redEdge, NIR)	5.5 cm	11 and 15 September 2021	70 m
		Sony A6000 (24 MP) with 21-mm Voigtländer lens	RGB	1.3 cm		

The hyperspectral data for study **I** were collected using a Fabry–Pérot interferometer (FPI) sensor in both leaf-off and leaf-on conditions. The sensor captured images in 36 bands from 500–900 nm, with dimensions of 1,024 × 648 pixels. Additionally, an RGB camera was mounted on the drone. The weather conditions varied from cloudless and bright during leaf-off data collection to sunny and cloudy during leaf-on data collection. The drone flew at a speed of 3 m/s with forward and side overlaps of 83% and 80% for FPI camera blocks, and 96% and 85% for RGB camera blocks, respectively. Georeferencing of the orthomosaics was achieved using 20 circular ground control points (GCPs) 30 cm in diameter. The coordinates of the GCPs were measured with a Trimble R10 (L1 + L2) RTK-GNSS receiver, providing horizontal and vertical accuracies of 2 cm and 3 cm, respectively. Reflectance calibration was conducted using 1×1 m reflectance panels placed near the drone's take-off location, along with irradiance measurement using an analytical spectrum device (ASD Field Spec Pro) with cosine collector optics.

The multispectral drone images for study **IV** were collected using a MicaSense MX Red-Edge sensor mounted on a quadcopter drone. The drone was equipped with a post-processed kinematic-level GNSS positioning system to georeference the images and a downwelling light sensor (DLS) to measure the illumination differences between images collected during flight. Additionally, an RGB camera was mounted on the drone. To ensure consistency between the RGB and multispectral data, the cameras were synchronized and captured images simultaneously. Additionally, a 50% reflectance panel from the MicaSense camera kit was used for every flight to establish the proper level for reflectance. The data collection took place over two days under cloudy or slightly overcast weather conditions. Reflectance panels and DLS were used to account for the overcast conditions, as per the MicaSense instructions. The reflectance panels were strategically placed in each flight to account for illumination conditions and prevent shadows or distortions. In order to obtain two baseline measurements and monitor changes in lighting conditions during the flight, images of the reference panel were captured just before and after each flight. The light conditions of each image were automatically stored by the DLS. The drone flew at 8–9 m/s at 70 m above the ground, with forward and side overlaps of 80% and 75% for MicaSense and 85% and 80% for RGB images, respectively. The data were collected from five flight zones, each covering approximately 10 ha.

In study **II**, mALS data were collected using three channels: at 532 nm, 1,064 nm, and 1,550 nm. The ALS systems used in study **III** were the SPL and LML systems, which employ nutating mirror palmar and rotating polygon scanning mechanisms, respectively. The point density of the SPL data decreases at the flight nadir and increases toward the edge of the flight lines due to its scanning mechanism. As described in Section 1.3.2, the SPL system sends and receives each sunbeam's backscattered laser signal using an array of 10×10 collimated sunbeams (Bernard et al. 2019), resulting in a similar or higher point density compared to the LML system. This higher point density was achieved despite the SPL system being collected from a flight height 2.6 times higher than that of the LML system. Both systems were planned to nominally collect 8 points/m^2. Table 2 provides a summary of the different ALS data collected for studies **II** and **III**, including details such as the wavelengths used, the scanning mechanisms employed, and the planned point density for each system.

2.4 Methodological overview

*2.4.1 Preprocessing of drone imagery data (studies **I** and **IV**)*

The preprocessing of drone data in studies **I** and **IV** involved creating dense point clouds from RGB images and creating image orthomosaics from hyperspectral (study **I**) and multispectral drone data (study **IV**). An overview of the entire methodological process for studies **I**–**IV** in this thesis is presented in Figure 3.

Figure 3. This flowchart provides an overview of the methodological steps conducted in studies **I–IV**. Each arrow type indicates the steps undertaken by its respective study, annotated with the study number near the top of the flowchart, under the icons depicting drone imaging (left) and airborne laser scanning (right).

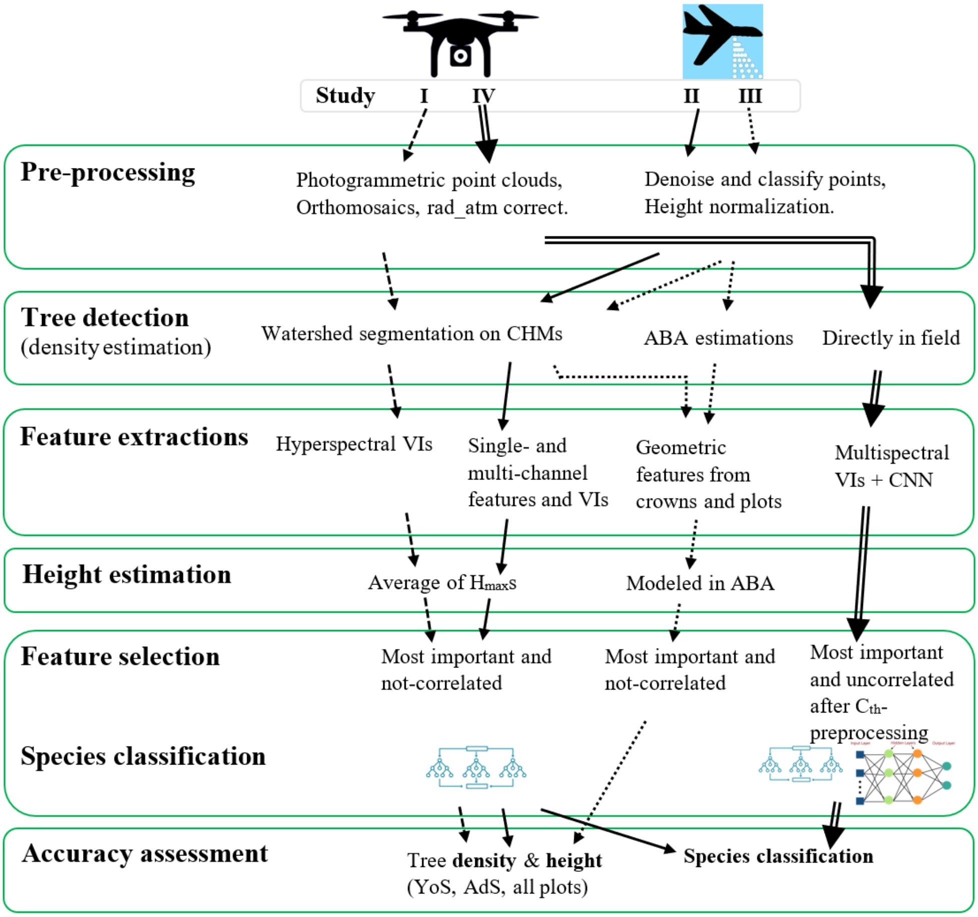

In study **I**, RGB images were georeferenced and processed using Pix4DMapperPro software to create dense photogrammetric 3D point clouds. Additionally, the FPI hyperspectral data were oriented and processed using a rigorous 3D approach (Nevalainen et al. 2017) for band co-registration and radiometric correction. This involved using radBA software (version 2016-08-20, Masala, Finland) for sensor correction, atmospheric correction, and normalization of directional dependency effects (Honkavaara et al. 2013; Honkavaara and Khoramshahi 2018). The final outputs were RGB and hyperspectral orthomosaics with specific ground sampling distances of 2.5 cm and 10 cm, respectively.

In study **IV**, the pre-processing of drone data began by geolocating the captured images using onboard Rinex GNSS log data from Trimble Virtual Reference Station with RTKLIB, version 2.4.3 b02 (www.rtklib.com, accessed on 10 October 2021) software. Subsequently, the accurate orientation and rotation of the images were determined using photogrammetric adjustment in Agisoft Metashape version 1.7. The datasets from RGB and MicaSense cameras were processed separately. The images underwent radiometric and geometric calibration to ensure accurate orientation and positioning. Dense point clouds were created from the RGB images, while multispectral data were used to generate multispectral orthomosaics. Notably, no GCPs were used, as the RGB camera system was already geometrically calibrated. Finally, RGB-based point clouds were generated at a 3-cm point distance, multispectral orthomosaics were created at a 5-cm resolution, and a 3-m resolution digital surface model was employed to mitigate possible distortions of trees.

Next, in study **I**, the heights of RGB point clouds were normalized to the ground height using a 2-m DTM created by the National Land Survey of Finland using ALS data updated in August 2015. Similarly, in study **IV**, this process was performed using the ground-classified laser returns from drone-laser scanning data collected on the 10^{th} of September 2021 at the flight height of 55 m and speed of 5 m/s, to provide a planned point density of >700 points/m^2.

*2.4.2 Preprocessing of ALS data (studies **II** and **III**)*

In studies **II** and **III**, the preprocessing of ALS data involved classifying ground versus non-ground laser returns, followed by height-normalizing the ALS point clouds using the ground laser returns.

For the mALS data in study **II**, the classification of ground and non-ground (vegetation) laser returns was carried out using a standard procedure in TerraScan (TerraSolid Oy, Helsinki, Finland). The data were then cleaned of any potential noisy laser returns originating from beneath the ground surface or above the tree canopy. Subsequently, a triangulated irregular network formatted DTM was created using the ground-classified laser returns of three channels independently to prevent any potential difference between the channels of mALS data. The DTM was used to normalize the height of point clouds by subtracting the terrain height from the point cloud height. These preprocessing steps were conducted independently for both leaf-on and leaf-off data. The intensity of laser returns was used without calibration.

Similarly, in study **III**, the ALS data were initially preprocessed by the data provider (Leica Geosystems) using HxMap software (Leica HxMap 2022). Their preprocessing included noise removal from the data, which was adjusted for each sensor of LML and SPL. Next, laser returns from the ground were classified using the approach presented by Axelsson (2000), followed by creating a DTM using the Delaunay triangulation method. The height of point clouds was then normalized as in study **II**. Finally, laser returns from flight line overlapping areas were dropped to ensure the uniformity of the data to be used in the next steps. These steps were conducted separately for each SPL and LML dataset.

*2.4.3 Tree detection (studies **I**, **II**, and **III**)*

In studies **I**, **II**, and **III**, ITD and ABA methods were used to estimate tree density at the plot level. The ITD method involved creating canopy height models (CHMs) from drone-PPC or ALS data, with subsequent gap filling and smoothing CHMs, followed by watershed segmentation to detect tree crown boundaries. In study **IV**, CHMs were created from drone-PPC and used for further image pre-processing. Additionally, field-mapped trees were used to create image cubes for segment boundary definition, focusing on tree species classification.

In study **III**, methodological improvements were developed for ABA by combining ITD features with ABA (in the ABA_{ITD} method) and correcting edge-tree effects (in the ABA_{Edge} method); we named this approach the $ABA_{ITDedge}$ method. The ABA methods involved statistical modeling between relevant features, as well as field-measured tree density and height, using an ordinary least squares (OLS) regression model.

2.4.4 Feature extraction

The extraction of relevant features from different datasets was a key focus across all studies (**I**–**IV**). In study **I**, the primary analysis involved extracting features from hyperspectral images and calculating the mean and maximum height (H_{mean} and H_{max}) of each segment from the CHMs. The H_{max} values were used to identify and remove segments below specific canopy height thresholds (C_{th})–0.5 m and 1.0 m in YoS and AdS, respectively–based on the literature (e.g., the use of 0.5 m by Næsset and Bjerknes 2001; Økseter et al. 2015) and experimental validation. Next, after visual inspection and expert knowledge, pixels inside segments with ≥50% of H_{max} of each segment were kept to minimize the possible reflectance of the understory within each remaining segment. Additionally, the arithmetic mean of spectral values of each band was extracted from each segment and used to calculate the normalized difference vegetation index (NDVI), as the popular vegetation indices (VIs).

In study **IV**, a detailed feature extraction approach was employed, involving the creation of tensors (image cubes, the 10×10-pixel cubes centering the location of the field-mapped seedling treetops) from multispectral images. The C_{th} of pixels above 0.4 m were applied, and the dataset named withC_{th}, keeping the original data (on which the C_{th} operation was not performed) and naming them as noC_{th}. Study **IV** then included the extraction of various statistical handcrafted features from the spectral bands, such as minimum, maximum, standard deviation, range, and percentiles, and the calculation of eight different VIs for each of the extracted features. Given that the CNN methods of species classification necessitate tensors that are without null pixels, which arise as a result of nullifying the pixels below the C_{th}, these nulls were filled by employing 3×3 moving kernels around the gaps to fill them with the average of the eight closest pixels. The CNN method also automatically extracted features from the input 3D tensors, with and without the incorporation of VIs (named the withVIs and noVIs datasets, respectively), to explore the importance of VIs in CNN methods.

In studies **II** and **III**, various relevant features were extracted from the mALS and the SPL and LML datasets, including the extraction of intensity-related features from laser returns and the calculation of geometric characteristics and other relevant features for tree density and height estimation. The features in study **II** included H_{max}–the height of the highest laser return of all channels in each segment–and 208 intensity-related features extracted from the intensity values of laser returns of each channel above 6 C_{ths} (0, 0.2, 0.4, 0.6, 0.8, and 1 m). Next, the features were grouped into single-channel intensity (SCI) and multi-channel intensity (MCI) features. The MCI features were calculated by applying different VIs on the SCI features. As a result, a total of 78 SCI features and 130 MCI features were extracted from laser points above each of the six C_{th} per segment, yielding six separate datasets. In study **III**, a comprehensive set of geometric features was extracted from each sample plot and ITD segment, utilizing all the laser returns from the SPL and LML datasets. Next, the features were grouped into features suitable for tree density and height estimation.

Furthermore, in study **III**, methodological improvements were applied for the $ABA_{Ordinary}$ method, including the correction of edge-tree effects (ABA_{Edge}), integration of ITD features (ABA_{ITD}), and introduction of a new combined approach ($ABA_{EdgeITD}$) to enhance the estimation of tree density and mean height. These methods involved extending or shrinking the plot boundary based on the H_{max} of the segment boundary falling inside or outside of the plot (ABA_{Edge}), adding plot-level averaged ITD-derived features to the $ABA_{Ordinary}$ features (ABA_{ITD}), and combining the two methods, respectively.

Overall, the feature-extraction process in the studies involved a range of techniques tailored to the specific characteristics of the input data, and the extracted features were utilized for tree density and height estimation in the respective studies. The plot-level tree density in all studies involved the calculation of the number of detected trees within the plot area, followed by the conversion of the area to hectares.

2.4.5 Tree height estimation

The H_{max} values extracted from each segment were utilized as estimated tree heights, and the arithmetic means of these H_{max} values were calculated to estimate mean tree height at the plot level using the ITD methods in studies **I** and **II**. In study **III**, the mean tree height was estimated through statistical modeling of the extracted ABA features and the field-measured mean tree height. It is important to note that study **IV** did not include tree height estimation as part of its focus.

2.4.6 Feature selection and tree species classification

The feature selection and tree species classification procedures in the respective studies were conducted with specific methodologies tailored to the unique characteristics of the datasets. In study **I**, a visual interpretation was performed to select and label training segments, followed by the selection of the most important features for distinguishing trees from non-trees and spruce from birch. The RF classifier was implemented to identify the optimal features, and the selected features were used to predict the classes of each segment. However, the species classification accuracy was not reported due to limited training data.

Similarly, in study **II**, a visual interpretation was conducted on the ALS-derived segments, and a larger number of training and validation segments were labeled. It included two separate and independent datasets created from segments inside (for training) and outside (for assessing the species classification accuracy). The feature importance was determined using the RF classifier, and the most important and uncorrelated features ($r < 0.8$) were selected for the classification of segments after being grouped into different intensity groups of features. Finally, the RF was trained to predict the classes of the segments using the most important and uncorrelated features of all three channels (MCI), as well as using features of SCI-Ch_1 and SCI-Ch_2, as single-channel ALS systems most frequently employ these wavelengths (Budei et al. 2018). Each process was conducted identically and independently for each dataset.

In study **III**, an extensive feature selection process was undertaken to select the optimal inputs for OLS linear regression models to estimate plot-level tree density and heights using different ABA methods. The feature selection involved finding features with maximal correlation with the target variables and addressing intercorrelations between the selected features ($r < 0.8$). Once the normality assumption of linear regressions was checked, an independent regression model was trained and validated on each dataset through a 5-fold leave-one-out cross-validation (LOOCV) approach to avoid overfitting and assess the accuracy of the regression models. Then, the regression model with the lowest prediction error was used for predicting all the data outside of the LOOCV approach.

In study **IV**, the training phase of the RF classifier was hypertuned using a 5-fold LOOCV implemented in grid search functionality in the scikit-learn library in Python (Pedregosa et al. 2011), and the feature importance was extracted from the best model. The five most important and uncorrelated ($r < 0.8$) features were selected for seedling species classification using the RF classifier. In this study, the 5,417 field-located species classes were randomly split into training (80%), validation (10%), and testing (10%) datasets, which were used in the same manner for all datasets and methods.

Furthermore, the main focus of study **IV** was to improve the classification of detected seedlings by adding C_{th}-based image preprocessing prior to feeding them into a sequential multi-layer perceptron CNN. The architecture of the developed CNN included specific components and activation functions to enhance the classification process. While default values were utilized in certain aspects of the CNN model, the dropout rates, dense units, and batch sizes were optimized through a Python code that exhaustively tested various combinations of values using a grid search. Each model combination was configured to iterate up to 300 times (epochs), and the computational efficiency was enhanced by customizing a callback function to implement early stopping if no improvement in validation accuracy was observed after 100 runs (patience = 100). Additionally, the model was programmed to save the progress when the validation accuracy of an epoch increased compared to the previous epoch. The computational efficiency was improved by parallelizing in Python to run on 7 single-nodes (10 CPUs) in the Puhti supercomputer provided by the CSC – IT Center for Science Finland (2022).

In study **IV**, after training the best models of the CNN and RF on the training datasets withC_{th} and noC_{th} separately, these models were utilized to predict the species of test datasets that had not been previously observed by the models. Furthermore, to investigate the potential benefits of combining two classifiers trained on noC_{th} and withC_{th} datasets, the models were configured to predict the corresponding subset of the test dataset. Specifically, the model trained on the noC_{th} dataset was used to predict the species of the C_{th}-unaffected tensors in the test dataset (66.6%; 361 of 542 test tensors), while the model trained on the withC_{th} dataset was used to predict the C_{th}-affected tensors (33.4%; 181 of 542 test tensors). This process involved switching the subsets of predicted classes of each classifier without the need to retrain them. The underlying hypothesis was that the C_{th}-unaffected tensors in the test dataset would be more accurately classified by the model trained on the noC_{th} dataset, and vice versa for the C_{th}-affected tensors in the withC_{th} dataset. This expectation was based on the assumption that the most suitable parameters for each input dataset had been automatically selected during the hyperparameter tuning phase.

2.5 Accuracy assessment

The accuracy of the RS-based estimates was evaluated by comparing the results with corresponding field-measured data in all studies (**I**–**IV**). For tree density and height estimation in studies **I**, **II**, and **III**, absolute and relative root mean square error (RMSE) and bias were calculated (Equations 1–4), along with the Pearson correlation coefficient (*r*, Equation 5). The tree density and height estimates were analyzed among all plots as well as among the YoS and AdS plots in studies **I**, **II**, and **III**.

$$Bias = \frac{\sum_{i=1}^{n}(y_i - \hat{y}_i)}{n} \tag{1}$$

$$rBias(\%) = 100 \times \frac{BIAS}{\bar{y}} \tag{2}$$

$$RMSE = \sqrt{\frac{\sum_{i=1}^{n}(y_i - \hat{y}_i)^2}{n}} \tag{3}$$

$$rRMSE(\%) = 100 \times \frac{RMSE}{\bar{y}} \tag{4}$$

$$r = \frac{\sum_{i=1}^{n}(x_i - \bar{x}).(y_i - \bar{y})}{\sqrt{\sum_{i=1}^{n}(x_i - \bar{x})^2 . \sum_{i=1}^{n}(y_i - \bar{y})^2}} \tag{5}$$

where *n* is the number of field-measured plots, y_i is the field-measured value of the attributes of the question for plot *i*, $\hat{y}_i$ is the predicted value for plot *i*, and $\bar{y}$ is the mean of the attribute in the field data.

The species classification accuracy was assessed by overall accuracy (OA), recall, precision (studies **II** and **IV**), and F1 score (study **IV**) (equations 6–10):

$$OA = \frac{\mathrm{TP} + \mathrm{TN}}{\mathrm{TP} + \mathrm{TN} + \mathrm{FP} + \mathrm{FN}} \tag{6}$$

$$Kappa = \frac{2 \times (\mathrm{TP} \times \mathrm{TN} - \mathrm{FN} \times \mathrm{FP})}{(\mathrm{TP} + \mathrm{FP}) \times (\mathrm{FP} + \mathrm{TN}) + (\mathrm{TP} + \mathrm{FN}) \times (\mathrm{FN} + \mathrm{TN})} \tag{7}$$

$$Precision = \frac{\mathrm{TP}}{\mathrm{TP} + \mathrm{FP}} \tag{8}$$

$$Recall = \frac{\mathrm{TP}}{\mathrm{TP} + \mathrm{FN}} \tag{9}$$

$$F1 = 2 \times \frac{\mathrm{Precision} \times \mathrm{Recall}}{\mathrm{Precision} + \mathrm{Recall}} \tag{10}$$

where TP is true positive, TN is true negative, FP is false positive, and FN is false negative.

The classification accuracy was evaluated using all test datasets, as well as specifically for the C_{th}-affected tensors of the test dataset to further explore the assumptions that those tensors would be classified more accurately in the withC_{th} dataset compared to the noC_{th} dataset. For this analysis, the test dataset was split into 4 bins of 1–5, 5–20, 20–40, and >40% C_{th}-affection, keeping the unaffected tensors in the 5th bin. Additionally, the effect of seedling height on classification accuracy was investigated by grouping the observed and predicted species classes of the test dataset into 4 bins of <1.5, 1.5–2, 2–4, and >4 m using the field-measured height of the seedlings. To ensure the credibility of the results in these two further analyses, specific criteria were set for the number of observations in each analysis.

The tree density and height estimation in studies **I**, **II**, and **III** was conducted at the plot level, while species classification in studies **II** and **IV** was performed at the individual tree level. Therefore, all studies were assessed with their corresponding data from field measurements at the plot and tree level, respectively. The accuracy of tree density and height estimation was reported for all plots, as well as separately for YoS and AdS plots.

3 RESULTS

3.1 Estimating tree density

Table 3 provides a summary of the most accurate results of tree density estimation conducted in different studies of this thesis using different RS materials and methods.

In the Overall dataset, tree density was estimated more accurately when leaf-on drone-PPC data were used in study **I** for all trees (rRMSE of 26.8%) and spruce trees (28.1%) compared to that of the leaf-off condition (33.5% and 44.6%, respectively). However, mALS data used in study **II** yielded more accurate spruce density estimates when acquired in leaf-off condition (rRMSE: 37.9%) compared to leaf-on condition (57.0%). The tree density estimates reached an rRMSE of 64.9% using LML in study **III**, which was slightly more accurate (65.1%) than that of SPL.

Comparing tree density estimate accuracies in YoS and AdS plots, tree density was always more accurately estimated for AdS than YoS. For example, the tree density of spruces reached an rRMSE of 19.2% when using drone-PPC data collected in the leaf-on condition (study **I**) compared to 58.2% for spruces in YoS. The same trend was observed in all trees overall, reaching 22.3% and 32.7% in AdS leaf-off and YoS leaf-on, respectively. Study **II** also confirmed the observation that the tree density of spruces was more accurately estimated in AdS (6.2%) than YoS (46.5%), both using leaf-off data. It was remarkable that the rRMSE was over seven times more accurate in AdS than YoS in the mALS data used in study **II**. Furthermore, study **III** showed that the tree density of all trees was estimated more accurately in AdS (60.6%) than YoS (73.7%) in LML, similarly to that in SPL (61.5% and 72.3% for

Table 3. Summary of the most accurate tree density estimates assessed among young (YoS), advanced (AdS), and all seedling plots (Overall) in studies **I–III**. Numbers in each cell represent rRMSE% and rBias, respectively. The en dash ("–") signifies unassessed parameters.

Study number, material used	Growth stage	All trees		Spruce	
		Leaf-off	Leaf-on	Leaf-off	Leaf-on
I, Drone-PPC+hyperspectral	YoS	47.3, 38.8	32.7, 29.4	58.5, 53.8	58.2, 57.5
	AdS	22.3, 6.3	22.7, 15.4	34.6, 28.3	19.2, 12.7
	Overall	33.5, 17.5	26.8, 20.2	44.6, 37.1	38.1, 28.1
II, Multispectral ALS	YoS	–	–	46.5, 28.8*	78.5, 76.9
	AdS	–	–	6.2, 4.0*	18.3, 17. 7
	Overall	–	–	37.9, 23.4*	57.0, 44.8
III, SPL and LML	YoS	–	73.7, 39.7**	–	–
	AdS	–	60.6, 4.6**	–	–
	Overall	–	64.9, 10.1**	–	–
IV, Multispectral drone	–	–	–	–	–

***** The C_{th} for YoS, AdS, and overall was 0.4 m, 1 m, and 0.4 m, respectively.

****** Results from the LML dataset were selected due to smaller rRMSE overall compared to SPL in the ABA_{ITD} and $ABA_{EdgeITD}$ methods.

AdS and YoS, respectively). Tree density estimation was not assessed and reported in study **IV**.

Applying methodological improvements in studies **II** and **III**, including optimizing C_{ths} for extracting ITD features and advancing the ABA method by correcting edge-tree effects and adding ITD features, improved the accuracy of tree density estimation. For example, study **II** showed that it reached the most accurate estimation when using a C_{th} of 0.4 m for all and YoS plots (rRMSE: 37.9% and 46.5%, respectively) and a C_{th} of 1 m for AdS plots in leaf-off mALS data (rRMSE: 6.2%). The novel method of $ABA_{EdgeITD}$ developed in study **III** succeeded in improving the tree density estimation from an rRMSE of 69.8% to 64.9% (rBias: 17.2% to 10.1%) from $ABA_{Ordinary}$ to $ABA_{EdgeITD}$ in the LML dataset, and likewise for SPL (67.4% to 65.1%, respectively, although rBias slightly increased from 15.8% to 18.9%).

3.2 Estimating tree height

Table 4 presents the most accurate mean tree height estimates obtained in different studies of this thesis (studies **I**–**III**) for all, YoS, and AdS plots using different RS materials and methods.

In the Overall dataset, the mean tree height was estimated more accurately using leaf-on data collected via the drone-PPC data obtained in study **I** for all tree (rRMSE of 11.5%) and spruce trees (11.4%) than when using the leaf-off condition (23.0% and 21.7%, respectively). Similarly, mALS data used in study **II** provided more accurate mean tree height estimation of spruces when acquired in leaf-on condition (rRMSE: 10.8%) compared to leaf-off condition (18.9%) regardless of C_{th} used. The mean tree height estimation was nearly

Table 4. A summary of the most accurate mean tree height estimates assessed among young (YoS), advanced (AdS), and all seedling plots (Overall) in studies **I**–**III**. Numbers in each cell represent rRMSE and rBias, respectively. The en dash (“–”) signifies unassessed parameters.

Study number, material used	Growth stage	All trees		Spruce	
		Leaf-off	Leaf-on	Leaf-off	Leaf-on
I, Drone-PPC+hyperspectral	YoS	26.6, 24.6	9.2, 2.6	26.4, 24.6	9.6, -2.4
	AdS	21.1, 20.1	10.9, 8.3	19.8, 19.4	10.8, 8.7
	Overall	23.0, 20.8	11.5, 7.4	21.7, 20.2	11.4, 6.9
II, Multispectral ALS	YoS	–	–	$3.5, 3.5^{1*}$	$3.5, -1.8^{2}$
	AdS	–	–	$17.3, 17.0^{3}$	$8.3, 5.0^{4}$
	Overall	–	–	$18.9, 17.6^{5}$	$10.8, 6.9^{6}$
III, SPL and LML	YoS	–	26.1, -18.5**	–	–
	AdS	–	15.6, 1.0***	–	–
	Overall	–	16.3, 0.3***	–	–
IV, Multispectral drone	–	–	–	–	–

* Superscript numbers ^{1} to ^{6} indicate C_{ths} of 1 m, 0.8 m, 0.6 and 0.8 m equally, 0 m, 0.8 and 0.6 m equally, and 0.2 m, respectively.

** Results from the SPL dataset under the ABA_{ITD} method, due to smaller rRMSE.

*** Results from the LML dataset under the $ABA_{EdgeITD}$ method, due to smaller rRMSE.

unbiased (rBias: 0.0 to 1.1% and *r*: 0.9 to 1.0 among all methods and datasets) and reached an rRMSE of 16.3% using LML in study **III**, which was slightly more accurate (17.1%) than SPL.

Comparing the accuracy of mean tree height estimation between YoS and AdS plots, tree height was estimated more accurately in AdS (rRMSE: 15.6% in LML) than YoS (26.1% in SPL) in study **III**. Study **III** showed that mean tree height estimation reached the highest accuracy for YoS plots when using SPL data (rRMSE: 26.1% in ABA_{ITD} method), and for AdS plots when using LML data (rRMSE: 15.6% in ABA_{ITD} and $ABA_{EdgeITD}$ methods). This was similar to the mean tree height estimation of all species and of spruce trees conducted in study **I** when using drone-PPC data collected in the leaf-off condition, which reached rRMSEs of 21.1% and 26.6% for the all-species AdS and YoS, and 19.8% and 26.4% for the spruce-tree AdS and YoS, respectively. However, the mean tree height of all species and of spruce trees was estimated more accurately in YoS than AdS when using leaf-on data from drone-PPC in study **I** (rRMSE: 9.2% and 10.9% for all-trees YoS and AdS, and 9.6% and 10.8% for spruce-tree YoS and AdS, respectively). Similarly, mALS data in study **II** yielded more accurate mean tree heights of spruce trees for YoS than AdS in both leaf-off and leaf-on conditions (rRMSE: 3.5% and 8.3% in leaf-on and 3.5% and 17.3% in leaf-off condition for YoS and AdS, respectively) (Table 4). The mean tree heights of YoS plots were overestimated by 2.4%, 1.8%, and 18.5% in leaf-on data used in studies **I**, **II**, and **III**, respectively; the mean tree height was not assessed and reported in study **IV**.

The methodological improvements applied in studies **II** and **III**, including optimizing C_{ths} and enhancing the ordinary ABA method by adding ITD features and correcting edge tree effects, improved the accuracy of mean tree height estimates. For example, study **II** showed that tree height was most accurately estimated when using a C_{th} of 0.2 m for the Overall plots in leaf-on data (rRMSE: 10.8%) compared to other C_{ths} in both epochs in Overall. However, the results of the optimal C_{th} deviated in study **II** such that it reached more accurate estimates at C_{ths} higher than 0.6 m in leaf-off data for Overall, YoS, and AdS plots (Table 4), and C_{ths} of 0.8 m for YoS plots–as well as 0.0 m and 0.2 m for AdS and Overall plots, respectively–when using leaf-on data. The $ABA_{EdgeITD}$ method developed in study **III** was successful in improving the mean tree height estimation from an rRMSE of 17.4% to 17.1% (rBias: 0.8% to 0.5%) from $ABA_{Ordinary}$ to $ABA_{EdgeITD}$ in the SPL dataset, and likewise for LML (rRMSE: 19.5% to 16.3%, and rBias: 0.8% to 0.3%). The estimated mean tree height values using the $ABA_{EdgeITD}$ method were the most accurate among other ABA methods overall, although the values were close to those of ABA_{ITD}. The $ABA_{EdgeITD}$ and ABA_{ITD} methods provided more accurate estimates for AdS and YoS using LML and SPL data, respectively (Table 4).

3.3 Tree species classification

The overall results of study **II** showed that classification of spruce, birch, and non-tree classes was more accurate in mALS data acquired in leaf-off condition (OA: 96.8%) than in leaf-on condition (92.5%; Table 5). The results also showed that using MCI features yielded more accurate species classification results (96.7%) than using SCI-Ch_1 (87.4%) and SCI-Ch_2 (82.8%) features, all based on leaf-off data.

The overall results of study **IV** showed that classification of the detected seedlings into pine, spruce, birch, and other species classes was more accurate using CNN (79.9%) than RF

Table 5. A summary of the maximum tree species classification accuracies achieved in studies **II** and **IV**. Numbers in each cell represent overall accuracy (%). The en dash (“–”) signifies unassessed parameters.

Study number and material used	Leaf-off	Leaf-on
I, Drone-PPC+hyperspectral	–	–
II, Multispectral ALS RF-classified birch, spruce, and non-trees	96.7%*	92.5%**
III, SPL and LML (ABA)	–	–
IV, Multispectral drone CNN- and RF-classified pine, spruce, birch, and other trees	–	79.9%***

* Refers to classification using MCI data at a C_{th} of 0.8 m.

** Refers to classification using MCI data at a C_{th} of 1.0 m.

*** Refers to classification using withVIs and a combined dataset classified using the CNN method. This reached 68.3% in RF using the withC_{th} dataset.

(68.3%). Pine seedlings were classified more accurately in CNN (recall: 0.6) than in RF (recall: 0.3% for the withVIs dataset). Moreover, fusing VIs into multispectral tensors assisted CNN to classify seedlings more accurately than not fusing VIs, e.g., 79.3% and 75.1% for the withC_{th} dataset, respectively.

The methodological development in study **II**–which aimed to minimize the intervention of laser returns from the understory by optimizing the C_{ths}–succeeded in improving the species classification. The development showed that an increase of C_{th} improved the OA in both leaf-off and leaf-on mALS data. For example, an increase of C_{th} from 0.0 m to 0.8 m improved the OA from 83.7% to 96.7% in leaf-off data; likewise, an increase from 0.0 m to 1 m improved the OA from 77.9% to 92.5% in leaf-on data. The effectiveness of this development was also observed when classifying seedlings using only features from SCI-Ch_1 and SCI-Ch_2. For example, seedling classification reached maximal accuracy at a C_{th} of 1.0 m for the leaf-off data (OA: 87.4% and 82.8% in SCI-Ch_1 and SCI-Ch_2, respectively), versus at a C_{th} of 0.0 m (58.9%) and 0.2 m (69.5%) for the leaf-on data using SCI-Ch_1 and SCI-Ch_2, respectively.

The development of a C_{th}-based image pre-processing method in study **IV** improved the OA of the C_{th}-affected subset of the test dataset (33.4%). For example, it improved OA among the C_{th}-affected subset of the test dataset from 75.7% to 78.5% in the CNN withVIs dataset, from 72.4% to 73.5% in the CNN noVIs dataset, and from 61.3% to 64.1% in RF. Further analysis on the C_{th}-affected test tensors showed that the OA was highest when they were C_{th}-affected by 1–5% and lowest when C_{th}-affected by >40% in both the noVIs and withVIs datasets. The developed method also remarkably improved the OA from 59.4% (original, i.e., noC_{th}) to 71.9% (processed, i.e., withC_{th}) on the >40%-affected bin with the noVIs dataset. The results of study **IV** also showed that the OA was higher when seedlings were taller than 1.5 m. For example, the OA was at least 82.4% among seedlings in all bins of above 1.5 m in the noVIs withC_{th} dataset, while it was 60% among seedlings in the bin that included seedlings shorter than 1.5 m. Overall, the developed method improved OA in RF (from 67.9% to 68.3%) and in CNN withVIs (79.0% to 79.3%), while it reduced the OA slightly in the noVIs dataset (by 1.8 percentage points (pp); 76.9% to 75.1% in noC_{th} and withC_{th}, respectively).

Combining subsets of the test dataset predicted by individual models of the withC_{th} and noC_{th} datasets in study **IV** improved the OA in the C_{th}-affected subset of test datasets in CNN. The OA reached 83.3% in tensors affected by 1–5% in withVIs. Regarding the OA in different seedling height bins, the combined method also improved OA in all bins, similar to what was observed for the individual datasets. Overall, the combined method improved OA in CNN (in both the withVIs and noVIs datasets). For example, it improved OA from 79.0% (noC_{th}) and 79.3% (withC_{th}) to 79.9% (combined) in the withVIs dataset, with a similar pattern observed for noVIs. However, in the RF method, the combined method caused a reduction in OA to 66.6% from 67.9% (in noC_{th}) and 68.3% (in withC_{th}).

Although species classification was conducted in study **I**, the species classification accuracy was not assessed and reported due to the small number of training data that were visually annotated.

4 DISCUSSION

4.1 Seedling tree density can be estimated using remote sensing

4.1.1 Comparing estimation accuracy with the state of the art

Our findings indicate that RS methods can offer reliable tree density estimation in seedling stands. For instance, in study **I**, a leaf-on drone-PPC analyzed with the ITD method achieved an rRMSE of 26.8%, representing an improvement over the state-of-the-art accuracy reported in similar studies in seedling stands. The studies utilized drone-PPC or ALS data processed with either ABA or ITD methods. For example, Puliti et al. (2019) employed both PPC and ALS data processed with the ABA method, resulting in rRMSE values of 36.3% and 53.4%, respectively. Additionally, Närhi et al. (2008) and Rana et al. (2023) achieved rRMSE values of 45% and 41–92%, respectively, in height estimation of seedling stands using operational nationwide ALS data (at 0.5 points/m^2, and 0.5 and 44 points/m^2, respectively) in Finland.

In study **II**, dense point clouds from mALS processed with the ITD method achieved an rRMSE of 37.9% for the overall tree density of spruces. The observed improvement in our studies **I** and **II** could be attributed to various factors, including the use of different methods (e.g., ABA vs. ITD), variations in input data quality (e.g., ALS vs. PPCs, point density, etc.), and differences in study designs (e.g., number of plots, forest conditions, etc.).

4.1.2 Effects of seedling stand development stage

The findings revealed that the developmental stage of seedling stands had a notable impact on the accuracy of tree density estimates. Across studies **I**–**III**, the estimates consistently exhibited higher accuracy in AdS compared to YoS, with respective rRMSE values of 22.3%, 6.2%, and 60.6% for AdS and 32.7%, 46.5%, and 73.7% for YoS. These values indicate that the most accurate results for AdS were achieved by mALS (study **II**), while drone-PPC in study **I** outperformed other methods for YoS (study **I**).

The superior performance of mALS for AdS can be attributed to the denser point clouds and the ability of ALS to penetrate the canopies of relatively dense AdS plots. Conversely, the use of drone imaging was more effective for detecting YoS than mALS due to the narrow laser footprints of ALS having a lower chance of hitting the treetops of small seedlings with less foliage and sharper treetops, particularly after thinning of the field plots to pre-defined densities in studies **I** and **II**. Another contributing factor to this trend may be the difference in tree heights between AdS and YoS, with the shortest tree in the field dataset of study **II** measuring 1.6 m in AdS and 0.7 m in YoS. Future studies could explore the use of mALS in unthinned YoS to validate the results obtained in thinned YoS stands.

The lowering of the C_{th} resulted in overestimation in YoS and increased the influence of understory reflectance, while raising it led to the omission of many seedlings from detection. Based on the findings, it may be appropriate to utilize a C_{th} of 1 m for seedling stands taller than 1.5 m.

4.1.3 Comparing leaf-off and leaf-on epochs

The comparison of leaf-off and leaf-on data collected in studies **I** and **II** revealed that in study **I**, leaf-on drone-PPC data yielded more accurate tree density estimates than leaf-off data, while in study **II**, leaf-off mALS data provided more accurate spruce tree density estimates than leaf-on data. This suggests that leaf-on drone imagery may be suitable for surveying seedlings due to its ability to provide spectral information for characterizing vegetation and seedling properties, including seedling health. However, for the specific purpose of detecting coniferous seedlings, leaf-off mALS data may also be appropriate.

4.1.4 Comparing remote sensing technologies (sensors)

The comparison of RS technologies for estimating tree density in seedling stands, as demonstrated in studies **I** and **II** using drone-PPC and mALS, yielded similar results (38.1% and 37.9% rRMSE, respectively). These findings align with other studies utilizing drone-PPC with ABA (rRMSE: 36.3% in Puliti et al. (2019)) and ALS with ABA (53.4% in Puliti et al. (2019), and 42% in Næsset and Bjerknes (2001)). Drone-PPC has been highlighted as the optimal tool for tree density estimation in mature forests (Puliti et al. 2020) and is favored by practitioners due to being a better-understood and more cost-effective solution than ALS (White et al. 2013b; Fassnacht et al. 2017). The comparable accuracy between passive drone-PPC and active mALS data underscores the superior capability of dense mALS, which can penetrate the canopy independently of direct sunlight and clear sky. However, mALS lacks detailed spectral characterization crucial for studying other seedling properties, such as seedling health. Therefore, each technology offers distinct advantages, and no single solution was identified.

Furthermore, the comparison of SPL and LML in study **III** revealed generally similar tree density estimates, with slightly lower underestimation in LML (10.1%) compared to SPL (18.9%) using the $ABA_{EdgeITD}$ method. This discrepancy reflects the advantage of SPL, captured at a higher flight height (3.75 km) than LML (1.45 km), making it a cost-efficient and faster option for nationwide forest inventorying, providing denser point clouds (10–100 times) than LML at the same flight height (Yu et al. 2020). Previous studies in mature forests have also recognized SPL's advantage in predicting species-specific tree volume (Räty et al. 2022) and forest attribute estimates (Yu et al. 2020), despite yielding similar or greater estimation errors. Another factor contributing to SPL's comparability with LML for seedling density estimation in study **III** is its higher point density (19 points/m^2) compared to LML (12.5 points/m^2; Table 2), with most laser returns being first or single returns from the top of the canopy, resulting in fewer gap-pixels in the generated canopy height models compared to LML.

4.1.5 Comparing effects of methodological developments on tree density estimation

Based on the findings of this thesis, the ITD method generally demonstrated higher accuracy in estimating tree density, particularly when dense point clouds were available, allowing for the detection of single trees. In contrast, the accuracy of tree density estimation using the ABA method, as reported in the literature (e.g., Næsset and Bjerknes 2001; Puliti et al. 2019; Rana et al. 2023; study **III**), was generally lower (rRMSE: 36.3–92%) compared to studies **I** and **II**, which utilized the ITD method (rRMSE: 26.8–37.9%). It is worth noting that the studies employing the ITD method had lower tree density in field plots, and that both methods can reach a saturation point, resulting in underestimation–particularly when tree density exceeds a specific value (e.g., 6,000 trees per hectare, not shown in the findings of study **III**). Despite the lower accuracy of tree density estimation using the ABA method, it still outperformed the NFI-based results of seedling density estimation reported in Rana et al. (2023) (rRMSE: 65–115%).

Furthermore, the development of the $ABA_{EdgeITD}$ method in study **III** indicated that incorporating single tree features and addressing edge-tree effects in the $ABA_{Ordinary}$ method improved tree density estimation from an rRMSE of 67.4% to 65.1% (SPL) and 69.8% to 64.9% (LML), with a similar trend in underestimation, except for the $ABA_{EdgeITD}$ method with SPL data. Despite attempts to improve the $ABA_{Ordinary}$ method and the utilization of novel high quality ALS data, the improvement was marginal in the magnitude of the accuracy of the study (rRMSEs of 65–70%), and it remained challenging to use ALS features extracted in the ABA method of tree density estimation. This challenge in predicting tree density using ALS in the ABA method was also noted by Næsset and Bjerknes (2001) and Puliti et al. (2019), as ALS point clouds are primarily used for height estimation rather than density estimation in ABA. These results were consistent with the plot-level estimation of Ørka et al. (2016) (rRMSE: 63.1%), but less accurate than those of other studies, such as Puliti et al. (2019), which achieved a plot-level rRMSE of 53.4% using ALS data in ABA. It is acknowledged that the regression modeling in study **III** omitted the consideration of tree species proportion in each plot to focus on presenting the main research development ($ABA_{EdgeITD}$).

The optimization of the C_{th} method in study **II** revealed that using C_{th} values of 0.4 and 1.0 m resulted in the most accurate tree density estimation for YoS and AdS, respectively. The findings aligned with the C_{th} values used in study **I** (0.5 and 1.0 m for YoS and AdS, respectively). Similarly, a C_{th} of 0.4 m was applied across all plots in study **III**, consistent with the C_{th} values (0.4 m and 0.5 m) employed by Korpela et al. (2008) and Ørka et al. (2016) when using ALS to assess seedling vegetation and predict tree density in seedling stands in their respective studies.

4.2 Seedling height can be estimated using remote sensing

4.2.1 Comparing estimation accuracy with the state of the art

The findings from studies **I**–**III** indicate that RS methods can be used for estimating seedling height. In study **II**, the most accurate results (rRMSE: 10.8%, bias: 0.2 m; rBias: 6.9%) were obtained when utilizing dense mALS data with a C_{th} of 0.2 m in leaf-on condition. This represents an improvement over existing methods such as ALS (rRMSE: 15–32%, Næsset and Bjerknes 2001; Närhi et al. 2008; Puliti et al. 2019; study **III**) and drone-PPC (11.5–30.9%, Puliti et al. 2019; study **I**) for estimating seedling height at the plot level. Additionally, our study **II** results outperformed those reported by Hartley et al. (2020) (rRMSE: 18.5%) for height estimation of individual seedlings in a forestry trial using drone-PPC, although their drone-laser scanning results were more accurate (rRMSE: 5.9%). Furthermore, our results in study **II** (RMSE: 0.2 m) were more accurate than the RMSE of 0.4 m achieved by Gallardo-Salazar and Pompa-García (2020) using drone-PPC to estimate the tree-level height of pines in an orchard, despite their smaller underestimate (5.5×10^{-5} m).

When compared to literature reporting only height underestimation, our results (rBias: 6.9%) were more accurate using the mALS and ITD method in study **II**. For example, Vepakomma et al. (2015) and Goodbody et al. (2018) reported underestimates of 0.4 m and 0.6 m, respectively, while Solvin et al. (2020) and Albuquerque et al. (2021) reported underestimates of 9.7% and 13%, respectively, using drone-imaging and individual tree detection level. Ørka et al. (2016) showed a 4.7% underestimate of stand-level height of seedlings when employing ABA with sparse ALS point clouds (0.7 points/m^2). Korpela et al. (2008) also observed 20–40% underestimates when utilizing leaf-on ALS (6–9 points/m^2) and aerial imagery using ITD to characterize seedling vegetation in a complicated setting (with high seedling density and species classes). The use of denser mALS point clouds (57.2 points/m^2) in study **II** compared to the mentioned ALS studies (with point densities of 0.7–19 points/m^2) may have contributed to the improvement in accuracy, although other parameters such as the different methods used (ABA vs. ITD) and different study designs (number of plots, forest conditions, etc.) also had an impact.

4.2.2 Effects of seedling stand development stage

The accuracy of tree height estimation is influenced by the development stage of seedling stands, as revealed by the results of this thesis. For example, study **III** demonstrated higher accuracy in AdS (15.6%) compared to YoS (26.1%). However, the use of mALS in study **II** presented contrasting results, with YoS estimates being more accurate than those of AdS in both epochs. For instance, in the leaf-off mALS data, the rRMSE (and rBias) were 3.5% (3.5%) and 17.3% (17.0%) for YoS and AdS, respectively. This discrepancy arises from the separate determination of the best rRMSE and rBias for each C_{th} optimization, irrespective of whether it was the best for all plots. Notably, the optimal C_{ths} for YoS and AdS were 1 m and 0.6 m (and 0.8 m equally), respectively, versus 0.8 m for all plots. These findings suggest that mALS data can be effectively used for YoS in both epochs, particularly considering that study **II** focused on spruces, which have needles in both epochs.

The slight overestimation of seedling height in the leaf-on mALS and drone-PPC may have been caused by the small time lag between field and RS data collection. Furthermore, the overestimation of height in YoS plots in study **III** (by 18.5%) may have been due to the use of ABA instead of ITD, as well as the predominance of field data from AdS (80 out of

89 sample plots), causing the regression to converge toward the average field-measured height. Inaccuracies in tree density estimation and species classification could also lead to overestimating tree heights in YoS plots due to the presence of taller non-tree segments (e.g., tall bushes, deadwood, stumps, etc.). Conversely, the slight underestimation of seedling height, especially in AdS, could be due to the regression to the mean height value in study **III**. Additionally, the issues of the laser missing treetop hits and the occlusion of suppressed trees in studies **II** and **III** could contribute to the underestimation, particularly in unthinned and dense seedling stands, and especially where birch trees dominate the conifers. This challenge of tree occlusion has been recognized as a significant obstacle in the accurate estimation of tree height using laser scanning in mature forests (Wang et al. 2019). Hence, if feasible, employing mALS for height estimation is advisable. However, for studies primarily focusing on spruces, either epoch would be suitable for this purpose.

4.2.3 Comparing leaf-off and leaf-on epochs

The results of studies **I** and **II** indicate that leaf-on data provide more accurate tree height estimates in both drone-PPC and mALS data compared to leaf-off data. This finding is particularly significant as the comparison of leaf-off and leaf-on data in seedling stands is a relatively new area of study, and our results align with previous research in mature forests. For instance, Bohlin et al. (2017) recommended the use of leaf-on aerial imagery for more accurate height estimation of deciduous trees. Similarly, Bohlin et al. (2016) reported lower height estimation in leaf-off aerial image data when estimating the proportion of deciduous tree volume in a mixed-species forest using ABA.

However, literature utilizing ALS and ABA has arrived at the opposite conclusion, with leaf-off ALS data yielding more accurate estimates for forest attributes in mature forests (Næsset 2005; Ørka et al. 2010: Villikka et al. 2012; White et al. 2015). The poorer accuracy of leaf-off mALS data in study **II** may be attributed to tree height growth between mALS data collection and field data gathering (which occurred with a time lag of approximately 45 days), as well as misclassification of spruces in the ITD method used. Therefore, collecting drone-PPC data in leaf-on condition could be considered for surveying seedlings, as it not only yields more accurate height estimates, but also provides useful spectral information for characterizing vegetation and seedling health. Additionally, leaf-on drone-PPC facilitates 3D object reconstruction, particularly for tree branches in YoS, which may contribute to better height estimation.

Considering the technological advancements that enabled the installation of both sensors on a platform, flying in leaf-on condition can be considered for seedling detection from imagery and height estimation from ALS data.

4.2.4 Comparing remote sensing technologies (sensors)

The comparison of RS technologies for tree height estimation revealed that dense mALS data provided more accurate results (rRMSE: 10.8% in study **II**) compared to drone imaging (rRMSE: 11.5% in study **I**), both using the ITD method. However, the height estimation accuracy in study **III** was lower (16.3%, using the SPL and $ABA_{EdgeITD}$ method) than in studies **I** and **II**. Nonetheless, it was nearly unbiased (0.3%) compared to the biases observed in studies **I** and **II** (7.4% and 6.9%, respectively). This unbiased result may be attributed to the underestimation of the height of AdS plots canceling out the overestimation of YoS height estimates. Additionally, the one-year interval between field data acquisition (from April 28 to September 9, 2017) and laser scanning may have allowed for tree height growth, potentially offsetting the underestimation of mean tree height. The denser point clouds used in study **II** (57 point/m^2) compared to study **III** (19 points/m^2) could also contribute to the more accurate results.

When consulting the literature, it was found that each study using ALS or drone-PPC showed different values based on the method, data quality, and forest conditions. For example, rRMSE values ranged from 15–32% when using ALS (Næsset and Bjerknes 2001; Puliti et al. 2019; study **III**) and 11.5–30.9% when using drone-PPC (Puliti et al. 2019; study **I**) for estimating seedling height at the plot level. The advantage of ALS over drone-PPC for tree height estimation has been established in mature forests (Järnstedt et al. 2012; Puliti et al. 2019; Mielcarek et al. 2020), as it penetrates inside and between canopies and can provide accurate DTMs, while drone-PPC does not (White et al. 2013b). This advantage of dense ALS data is complemented by its capability to operate regardless of direct sunlight, cloud cover, or time of day.

Furthermore, when comparing SPL and LML technologies for height estimation in study **III**, the results showed that SPL data produced somewhat similar or more accurate estimates overall than those of LML data, particularly for YoS plots. The advantage of SPL in estimating the height of YoS plots may be due to its denser point cloud and larger percentage of first/only returns compared to LML. Even if the results were the same, the advantage of SPL is evident as it captures data at a higher flight height, making it a cost-efficient and faster alternative for large-area mapping. This advantage of SPL was also reported in mature forests, where SPL flights at higher altitudes yielded more accurate estimates of structural metrics (e.g., height, Yu et al. 2020) and species-specific tree volume (Räty et al. 2022).

4.2.5 Comparing effects of methodological developments on tree height estimation

The incorporation of ITD features and correction of edge-tree effects addressed by the $ABA_{EdgeITD}$ method developed in study **III** improved tree height estimation relative to $ABA_{Ordinary}$. The incorporation of ITD features and correction of edge-tree effects resulted in enhanced accuracy, as indicated by reduced rBias and rRMSE values. Notably, the improvement was more pronounced in the LML data, with rBias and rRMSE decreasing from 0.8% and 19.5% to 0.3% and 16.3%, respectively. The addition of single tree features (ABA_{ITD}) demonstrated more substantial improvements compared to only correcting edges (ABA_{Edge}), and the combination of both approaches yielded even more accurate estimates in SPL data. These methodological developments, particularly in the $ABA_{EdgeITD}$ method, represent a novel application in seedling stands, with few prior attempts having been made to enhance $ABA_{Ordinary}$ in mature forests. Our findings align with previous research on the use of ABA_{ITD} to improve height estimation in mature forests, such as the work by Hyyppä et al. (2012), further validating the efficacy of the approach.

In addition, the optimization of the C_{ths} in study **II** identified optimal C_{th} values for the height estimation of YoS and AdS (0.2 m, and 0.2 and 0.6 m, respectively), shedding light on the significance of tailoring C_{th} values to forest stands at different developmental stages. These findings differed from the C_{th} values used in study **I**, which were 0.5 m and 1.0 m for YoS and AdS, respectively. When considering all plots, the optimal C_{th} of 0.2 m was lower than the C_{th} of 0.4 m employed by Korpela et al. (2008). The lower C_{th} found in study **II** may be attributed to the accurate classification of the remaining tall spruces, which would raise the mean plot height. Notably, our optimal C_{th} of 0.2 m for height estimation closely aligned with the results of Ørka et al. (2016), who reported more accurate height estimation using a C_{th} of 0.0 m in regeneration forests. The comparison of our C_{th} optimization results with those in the literature emphasized the importance of optimizing C_{th} for each forest variable separately, as demonstrated by Gorgens et al. (2017) in mature forests. In study **II**, the underestimation of spruce density in leaf-on data resulted in slight (2.4%) height overestimation due to the omission of small spruces from detection. Therefore, this optimization was essential as it first affected tree detection (density estimation) and subsequently influenced height estimation.

Furthermore, the comparison of the ITD and ABA methods used for height estimation in studies **I**–**III** indicated that the ITD method generally provided less error (smaller rRMSEs in studies **I** and **II**), while ABA provided nearly unbiased tree height estimates in study **III**.

Note that the observed deviations in results across the studies underscore the complexity of drawing definitive conclusions, emphasizing the need for careful consideration of various influential parameters, including tree density in field plots and the quality of RS data. Nonetheless, the spatially explicit and tree-level height estimation provided by the ITD method offers distinct advantages over the plot- or stand-level estimation offered by ABA, highlighting the potential for tailored applications based on specific objectives and forest characteristics.

4.2.6 Other factors influencing height estimation

Several factors influenced the height estimation in this thesis, including the accuracy of the Näslund model and DTMs used to normalize the height of point clouds. The Näslund model predicted heights of YoS and AdS with rRMSE values of 12.8% and 11.8% and rBias values of -0.1% and 0.6%, respectively, in study **I**. Additionally, the accuracy of DTMs (approximately 0.1–0.3 m**)** had an impact on the height estimates, particularly for YoS in studies **I** and **II**, as small errors for shorter trees in YoS had a more significant effect than those in AdS height estimates. This also affected the estimation of tree density–especially for YoS, where trees are smaller and more vulnerable to changes in C_{ths}–in study **II**. Furthermore, Näslund's model would not be necessary if tree height were measured at the individual tree level during field surveys, and RS-assisted height estimates could be evaluated at the individual-tree and plot levels instead.

The height estimation in study **III** could also be improved by modeling YoS and AdS plots separately, or by separating them into different tree density bins if more field plots were available. This could potentially resolve the overestimation of YoS plot heights observed in study **III**. However, this approach would move the computations away from the operational level.

4.3 Species classes of seedlings can be distinguished using remote sensing

4.3.1 Comparing classification accuracy with the state of the art

In comparing our classification accuracies with those obtained using state-of-the-art methods, the results of the studies demonstrated the effectiveness of utilizing novel RS materials and methods of classifying seedlings. In study **II**, the use of mALS achieved an OA of 96.7% for classifying seedlings into spruce, birch, and non-trees, with a mean precision of 0.9%. Similarly, study **IV** utilized multispectral drone imagery with CNN and achieved an OA of 79.9% for classifying seedlings into pine, spruce, birch, and other species classes. These results surpassed the reported accuracy of other studies, such as the classification of grass, seedlings, and other classes in a restoration forest area in the Brazilian Atlantic forest, which achieved an OA of 75% using low-cost drone-RGB imagery (Albuquerque et al. 2021). Furthermore, studies using drone-RGB imagery for seedling classification reported average precisions of 0.9 (Feduck et al. 2018) and 0.8 (Fromm et al. 2019) for distinguishing coniferous seedlings from non-seedling objects. The superior accuracy of the findings in the current studies demonstrates the effectiveness of the utilized method and input data, particularly in classifying seedlings into multiple species classes.

A comparison with previous studies using different sensors for species classification of seedlings is crucial for contextualizing the performance of the novel mALS data used in study **II**. The OA–ranging from 24% to 71.8%–reported in previous studies using alternative sensors underscores the challenges and variability in seedling species classification. For example, Korpela et al. (2008) achieved an OA of 39% when using features from both ALS and aerial imagery to distinguish 27 classes from sunlit observations in seedling stands. They also noted that when utilizing only features from images or ALS, their OA decreased to 28% and 24%, respectively. Furthermore, Närhi et al. (2008) achieved a classification accuracy of 71.8% in spruce seedling stands using sparse (0.5 point/m^2) ALS data. In comparison to similar studies that used mALS to classify mature forests, the findings of Yu et al. (2017) are noteworthy for achieving slightly higher accuracy, with an OA of 86% in classifying pine, spruce, and birch trees.

4.3.2 Comparing leaf-off and leaf-on epochs

Comparing leaf-off and leaf-on mALS data in study **II** revealed that leaf-off data produced more accurate species classification (OA: 96.7%) than leaf-on data (92.5%). This finding is consistent with previous research that supported the advantage of leaf-off Optech Titan mALS data for the classification of mature trees, particularly coniferous species (Kim et al. 2009; Yu et al. 2017; Axelsson et al. 2018). Furthermore, Villikka et al. (2012) highlighted the advantages of employing leaf-off ALS data for ABA-based forest inventorying, particularly in scenarios requiring the differentiation between deciduous and coniferous trees. The outperformance of leaf-off data in study **II** could be attributed to the fact that coniferous trees, including spruce seedlings, remain green even in leaf-off data collection time, making species classification easier. Additionally, the commission of non-trees as spruces caused overestimation (by 23.4%) of spruce tree density in leaf-off data. Future studies could investigate each variable separately to eliminate the effect of tree detection accuracy on species classification accuracy. Therefore, the use of leaf-off mALS data could be more useful for species classification, especially if coniferous trees are the main species of interest.

4.3.3 Comparing remote sensing technologies (sensors)

Comparison of the RS technologies used in study **II** revealed that species classification accuracy was significantly higher when using MCI features from mALS data compared to SCI features from Channel 1 and 2 (SCI-Ch_1 and SCI-Ch_2). For instance, the OA reached 94.6% using leaf-off MCI data in C_{th} 0.6 and 0.8 m, while it was 84.8% and 81.5% using

SCI-Ch_1 and SCI-Ch_2, respectively. This observation aligns with similar findings in studies conducted in mature forests (Kim et al. 2009; Korpela et al. 2012; Yu et al. 2017; Axelsson et al. 2018; Budei et al. 2018). Furthermore, the results highlighted that employing MCI features from mALS data was potentially more reliable and beneficial for classifying smaller seedlings compared to using SCI-Ch_1 and SCI-Ch_2. mALS has been proposed as a potential single-sensor solution for species classification in mature forests (Yu et al. 2017) in boreal areas limited to three main species classes in Finland. Based on our findings in study **II,** it can be considered for use in classifying species of seedlings as well.

Additionally, the study demonstrated that species classification was more accurate when utilizing SCI-Ch_2 (OA: 69.5%) compared to SCI-Ch_1 (53.7%) in leaf-on data with a C_{th} of 0.2 m, possibly due to the increased reflectance of vegetation in the NIR wavelength in the leaf-on condition.

Adding VIs in study **IV** was somewhat similar to using MCI in study **II** from the perspective of adding new features for the classifiers. The results of study **IV** showed an improvement in OA when fusing VIs to the drone-multispectral imagery in the CNN method. The inclusion of VIs appeared to improve the performance of the data-hungry CNN methods, resulting in consistently higher OA in the withVIs dataset compared to the noVIs dataset. Other studies using satellite imagery (Worldview, Sentinel-2) to classify species of urban trees or mountainous protected areas have also observed a comparable improvement in OA by fusing VIs (Hartling et al. 2019; Yaloveha et al. 2021; Adagbasa et al. 2022).

Note that the species classification accuracy using drone-hyperspectral data was not reported in study **I**, preventing a direct comparison with the results using drone-multispectral data in study **IV**.

4.3.4 Comparing effects of methodological developments on tree classification accuracy

Comparison of the effect of optimizing C_{ths} to enhance species classification accuracy in study **II** revealed that increasing the C_{th} improved the accuracy by minimizing interference from ground and understory vegetation. The worst OA was achieved with a C_{th} of 0 m, indicating that employing a C_{th} method was beneficial for improving species classification accuracy in seedling stands.

A methodological development in study **IV** was the application of C_{th}-based image preprocessing on input tensors before feeding them to CNN and RF classifiers, which aimed to improve species classification. The results demonstrated a 2.8-pp improvement in species classification accuracy in C_{th}-affected tensors using the withVIs CNN method, as well as in the RF method. This improvement minimized interference from understory reflectance, particularly in shorter seedlings. The novelty of the proposed method in seedling stands necessitates a comparison of the findings with those reported in the literature on mature forests. Previous studies on mature forests have explored hybridizing the CNN and K-nearest neighbor (Prasad and Senthilrajan 2022), merging Res-Net and U-net (Chen et al. 2021), utilizing a 3D-1D-CNN approach (Zhang et al. 2020), and employing a new two-phase CNN (Ao et al. 2023). These studies reported improvements in OA ranging from 1 to 1.4 pp, which aligns with the improvement in seedling classification observed in study **IV**.

Further analysis of this method revealed that it was more successful in improving tensors C_{th}-affected by 1–5% compared to those C_{th}-affected by >40%. However, the method achieved a striking improvement (from OA 59.4% to 71.9%) in the "more challenging"

>40%-affected tensors, demonstrating its significance. Additionally, the OA of the method was higher (82.4%) among tensors taller than 1.5 m compared to shorter seedlings (60%).

Another methodological development in study **IV** involved merging subsets of the test dataset based on C_{th}-affected or unaffected status. This method further improved species classification accuracy in CNN for the withVIs and noVIs datasets. For example, in the withVIs dataset, the OA increased from 79.0% (noC_{th}) and 79.3% (withC_{th}) to 79.9% after applying this method. The improvement was more pronounced in C_{th}-affected tensors (from 75.7% to 78.5%), while the unaffected subset of test datasets saw a slight decrease in accuracy (from 80.6% to 79.8%). This method has the potential to aid seedling stand inventorying, aligning with previous research employing a similar methodology.

The findings of this method merging the subsets of the test dataset in study **IV** aligned with prior research in mature forests that utilized a similar approach. For instance, Martins et al. (2021) employed a multitask CNN with a post-processing step, akin to the method used in study **IV**, to classify tropical urban trees. Their approach resulted in an average F-score of 79.3 ± 8.6%, indicating improved species classification accuracy. Similarly, Anderson et al. (2023) found that combining CNN and object-based-image analysis (OBIA) techniques led to higher overall accuracy (91%) for classifying invasive species in wetlands using drone-based RGB data, compared to using CNN alone (88%). However, the results of study **IV** demonstrated that this merging method did not improve species classification accuracy in RF, likely due to the handcrafted features in the withC_{th} dataset not requiring the filling of nullified pixels.

4.3.5 Comparing classifiers (CNN and RF)

The findings from study **IV** demonstrated that species classification of seedlings achieved higher accuracy with CNN (79.9%) compared to RF (68.3%). This superior performance of CNN over RF aligns with similar studies in mature forests, where CNN outperformed RF by 4.4–38.6 pp (Raczko and Zagajewski 2017; Hartling et al. 2019; Xi et al. 2019; Zhang et al. 2020; Mäyrä et al. 2021; Ye et al. 2021; Adagbasa et al. 2022; Anderson et al. 2023). For example, Xi et al. (2019) reported that a one-dimensional CNN outperformed RF in tree species classification by 4.4 pp (OA: 85.0% and 80.6%, respectively) using OHS-1 hyperspectral satellite data.

Comparing the achieved OA of 79.9% in study **IV** with those reported in the literature on seedling stands, it is evident that the results of each study varied based on the input data, the classification model used, species composition, and forest conditions. For instance, in study **II**, seedlings were classified into spruce, birch, and non-tree classes using manually extracted mALS data intensity and classified with the RF classifier. The study achieved an OA of 96.7% in leaf-off data using a C_{th} of 1 m. However, the study did not include the pine class, and the results were obtained in leaf-off condition. Therefore, direct comparisons with other studies are limited, and the focus was on achieving the highest possible accuracy within each study.

The superiority of CNN to RF in study **IV** was evident in the accuracy of classifying each species class. The results showed that CNN was able to classify pine more accurately (recall: 0.6) than RF (recall: 0.3%) in the withVIs dataset. This finding was consistent with the research of Trier et al. (2018), who found that the classification of birch species was more accurate using CNN (86%) than their index technique (26%) using hyperspectral data.

Furthermore, the recall for the main tree species (pine, spruce, and birch) was more accurate (0.6, 0.8, and 0.9, respectively) than the recall of other species (0.5) because the other species classes were frequently misclassified as birch (e.g., recall of 0.5 in the withVIs dataset using the combined method). This was expected, since 99% of other deciduous trees and 1% of other coniferous trees belonged to the other species class. As a result, several seedlings from the other species class were classified as birch (recall 0.6).

While the OA could be improved by merging the other class into the major classes (birch and pine), the resulting estimates would not be suitable for operational use in forest inventorying. An alternative approach would be to combine the other classes into two new ones, such as other deciduous and other coniferous, but this would necessitate gathering more field data for the other species class.

4.3.6 Other factors influencing seedling classification

The results of study **IV** highlighted two key parameters that significantly impact the accuracy of species classification: 1) the proportion of C_{th}-affected pixels of a tensor, and 2) the height of seedlings. These factors collectively hindered the classification of seedlings, with the majority of tensors being more than 40% C_{th}-affected, representing trees shorter than 1.5 m. The findings demonstrated that classification of small seedlings (height < 1.5 m) and tensors affected by more than 40% C_{th} was challenging. However, the proposed C_{th}-based image preprocessing method enhanced the classification of shorter seedlings by up to 8 pp and tensors affected by more than 40% C_{th} by 12.5 pp. This preprocessing method proved to be particularly influential in improving the classification of very difficult seedlings.

The accuracy of classification was further improved for tensors in the 2–4 m and >4 m height bins, as these tensors had fewer nullified pixels, resulting in more accurate OA. Conversely, the results for trees larger than 4 m remained unchanged, as there were no nullified or C_{th}-affected pixels in their tensors. The tensors unaffected by C_{th} were generally classified more accurately compared to C_{th}-affected tensors in both datasets (withVIs and noVIs) and using both classifiers. This was expected, as the majority of C_{th}-unaffected tensors represented taller seedlings with denser foliage, minimizing the effect of the understory.

The size of the tensors was identified as an influential factor in species classification accuracy. For example, Zhang et al. (2020) and Sun et al. (2019) achieved more accurate tree species classification in mature forests using larger tensor sizes (13×13 and 64×64, respectively). However, in the context of study **IV**, such large tensor dimensions would include multiple seedling canopies or large understory reflectance due to the close spacing and smaller size of the seedlings, as well as the 5-cm pixel size of the multispectral data used.

Considering the rapid advancements in camera technologies that enable the collection of even finer-resolution (1 cm) imagery at the same flying heights as those used in study **IV**, future studies are likely to yield improved findings, especially for YoS in the near future.

4.4 Constraints and future steps

This thesis has considerably advanced the RS methods of characterizing seedling stands, particularly in estimating species-specific tree density and height. However, further research is needed to improve the performance and efficiency of these methods. Studies **I**–**III** were limited by the inclusion of a small number of field-measured plots and low variability in species and densities. Therefore, future studies should consider including a greater number of field sample plots with a wider range of tree densities, species, and heights. Additionally, utilizing tree-level field data would be preferable to plot-level field data, as it would allow for more detailed spatial results and greater reliability compared to methods such as the visual interpretation of species from drone images.

In future research, it is important to tackle challenges related to tree detection and species classification arising from thickets, particularly in seedling stands with clumped spacing. The presence of a few birches resembling grass or thickets alongside the conifer seedlings is a normal occurrence in tightly spaced seedling stands, impacting tree detection, height estimation, and species classification. In study **IV**, approximately 7% of the field data (tensors) exhibited impurity of species classes, indicating the presence of at least one other tree class beneath the canopy of the primary species of the tensor. This impurity posed challenges in the process of classifying tree species in study **IV**. Furthermore, the thicket seedlings posed challenges in detecting seedlings using aerial and drone imagery, as observed in previous studies by Hall and Aldred (1992) and Röder et al. (2018). For instance, Röder et al. (2018) reported a general tree detection rate of 39.1%, which decreased to 17.8% in thicket seedlings. This underscores the impact of thickets on seedling detection and emphasizes the importance of utilizing high-resolution RS data and innovative methods to address this issue. For example, the application of superpixel-enhanced CNN methods may offer a potential solution for improving seedling detection accuracy, as demonstrated in the detection of urban trees by Liu et al. (2023).

Further research is essential to enable large-scale operational applications that allow foresters to efficiently update data over extensive areas in a cost-effective and timely manner. One potential approach is the combined use of very high-resolution satellite imagery and drone-imagery.

The growing interest in utilizing shelterwood-based silvicultural systems to address climate change and biodiversity in Finland underscores the need for innovative research and methods for seedling stands. Addressing the obstacles posed by shelterwood for drone flights close to the ground requires novel solutions to ensure accurate data collection and analysis. Lopatin and Poikonen (2023) tested a two-phase drone scanning method to obtain sub-centimeter RGB images of seedlings, dedicating one flight for scanning obstacles and retention trees before flying at a height of 5–20 m. However, the use of modern drones capable of obstacle avoidance by flying under the canopy (Hyyppä et al. 2020) could present a more appealing RS technology for assessing regeneration under the main canopy in shelterwood systems.

Future research efforts could focus on developing and adopting methods to address various emerging needs of foresters, such as seedling establishment, seedling health and mortality monitoring, and moose- and snow-damaged seedling detection, among others. For example, ALS has demonstrated its effectiveness in detecting moose-damaged pine seedlings in boreal forests (Melin et al. 2015), while hyperspectral imagery has been utilized to assess the health of pine seedlings threatened by a fungal pathogen in a greenhouse (Haagsma et al. 2020). These issues are gaining importance in the context of climate change, forest fires, droughts, and insect damage affecting seedling stands.

Future studies could also focus on directly detecting and classifying seedlings from orthomosaics (e.g., using faster-RCNN) or dense point clouds from drone-based laser scanning (e.g., employing PointNet^{++}). Although previous attempts have been made to detect and count seedlings from drone imagery (Fromm et al. 2019; Chadwick et al. 2020; Pearse et al. 2020; Jayathunga et al. 2023; Lopatin and Poikonen 2023), species classification has been absent from many studies.

The method developed in study **IV** could be further examined and enhanced in future studies by testing different kernel-filling strategies and experimenting with different C_{th} values. Another potential approach, contingent upon the availability of additional field data, could involve training and predicting the classifiers on C_{th}-affected and C_{th}-unaffected subsets of the dataset separately. Furthermore, results could be improved by incorporating hyperspectral imagery and performing atmospheric correction on multispectral data. Finally, the employment of more sophisticated and deeper CNN architectures could potentially improve the results, although this would increase the computational load.

5 CONCLUSIONS

In order to ensure sustainable forest management and secure future wood supplies, it is essential to obtain accurate and detailed information for implementing silvicultural management of seedling stands. Currently, this information is primarily obtained through costly, time-consuming, and labor-intensive field visits. This thesis aimed to develop new methods and explore different RS data to complement or replace field visits, thus contributing to the cost-efficiency and sustainability of forest operations.

The objective of this thesis was to characterize seedling stands by estimating the tree density, height, and species classes of seedlings. Various high-quality drone and laser scanning data were utilized, including drone-PPC, drone-hyperspectral data, mALS data collected in leaf-off and leaf-on conditions, as well as LML and SPL laser scanning data and drone-multispectral data. Additionally, this thesis developed the C_{th} optimization method (study **II**), the novel ABA approach method ($ABA_{EdgeITD}$, study **III**), and the C_{th}-based image preprocessing method (study **IV**).

Overall, this thesis demonstrated that the use of high-quality RS data and developed methods notably improved the accuracy of characterizing seedling stands. The results showed that RS methods consistently provided more accurate results for AdS than YoS in studies **I**–**III**, with YoS posing resistant challenges. Consequently, RS methods can be efficiently utilized for inventorying AdS, while field visits remain essential for YoS. Considering data collection epochs, drone imagery is best collected in leaf-on condition, while mALS data collection is preferable in leaf-off condition.

Different RS technologies can serve specific purposes in characterizing seedling stands. Dense mALS data are particularly suitable for estimating seedling height, while drone-PPC is effective for accurately estimating tree density, especially for YoS. Furthermore, the use of SPL data, collected at higher flight heights, yielded comparable or superior estimates–especially in YoS–compared to conventional LML, making it a viable option for operational large-area ALS-based seedling inventorying. The results also showed that using MCI features from mALS data for classifying tree species was more effective and accurate than using only SCI-Ch_1 or SCI-Ch_2 (study **II**). Furthermore, fusing VIs to multispectral drone imagery enhanced the accuracy of species classification by 4.3 pp when employing CNN methods (study **IV**).

The optimization of C_{th} in study **II** emphasized the significance of customizing C_{th} for tree density and height estimation. An optimal C_{th} of 0.4 m and 0.2 m provided the most accurate overall tree density and height estimation, respectively. Furthermore, the findings suggested that an increased C_{th} generally led to improved species classification accuracy. The

$ABA_{EdgeITD}$ method improved the accuracy of estimating tree density, and the mean height of seedling stands (study **III**). It outperformed the $ABA_{Ordinary}$ method, resulting in more accurate estimates of tree density and mean height (which improved by 4.9 and 3.2 pp, respectively).

The C_{th}-based image preprocessing approach, proposed and developed in study **IV**, improved the species classification of seedlings by 2.8 pp by combining the C_{th}-affected and C_{th}-unaffected subsets of the test datasets. Further analysis revealed that the shorter and highly-C_{th}-affected seedlings, which posed analytical challenges, were classified more accurately as a result of the methods developed in study **IV**. The results also showed that CNN outperformed RF in the classification of species for seedlings by improving OA up to 13.3 pp and the classification accuracy of pines by 50 pp.

In conclusion, the utilization of both drone imagery and mALS data has demonstrated its reliability for the RS-based inventorying of seedling stands. The integration of the methodological improvements developed in this thesis further enhances the reliability and applicability of these resources. The findings of this study contribute to the advancement of accuracy and knowledge in RS applications for seedling stands. It is evident that RS technologies can offer dependable support and potential alternatives to traditional field surveys of seedling stands, thereby assisting precision forestry and silvicultural decision-making, and consequently promoting sustainable forest management.

REFERENCES

Aasen H, Honkavaara E, Lucieer A, Zarco-Tejada PJ (2018) Quantitative Remote Sensing at Ultra-High Resolution with UAV Spectroscopy: A Review of Sensor Technology, Measurement Procedures, and Data Correction Workflows. Remote Sens 2018, Vol 10, Page 1091 10: 1091. https://doi.org/10.3390/RS10071091

Adagbasa EG, Adelabu SA, Okello TW (2022) Application of deep learning with stratified K-fold for vegetation species discrimation in a protected mountainous region using Sentinel-2 image. Geocarto Int 37: 142–162. https://doi.org/10.1080/10106049.2019.1704070

Äijälä O, Koistinen A, Sved J, Vanhatalo K, Väisänen P (eds) (2019) Metsänhoidon suositukset. Metsätalouden kehittämiskeskus Tapio, https://tapio.fi/wp-content/uploads/2020/09/Metsanhoidon_suositukset_Tapio_2019.pdf

Akbari V, Solberg S, Puliti S (2021) Multitemporal Sentinel-1 and Sentinel-2 Images for Characterization and Discrimination of Young Forest Stands under Regeneration in Norway. IEEE J Sel Top Appl Earth Obs Remote Sens 14: 5049–5063. https://doi.org/10.1109/JSTARS.2021.3073101

Albuquerque RW, Ferreira ME, Olsen SI, Tymus JRC, Balieiro CP, Mansur H, Moura CJR, Costa JVS, Branco MRC, Grohmann CH (2021) Forest restoration monitoring protocol with a low-cost remotely piloted aircraft: Lessons learned from a case study in the brazilian atlantic forest. Remote Sens 13. https://doi.org/10.3390/RS13122401

Alzubaidi L, Zhang J, Humaidi AJ, Al-Dujaili A, Duan Y, Al-Shamma O, Santamaría J, Fadhel MA, Al-Amidie M, Farhan L (2021) Review of deep learning: concepts, CNN architectures, challenges, applications, future directions(74 sayfa olan, scaling problem için güzel ref ler var). J Big Data 8

Anderson CJ, Heins D, Pelletier KC, Knight JF (2023) Improving Machine Learning Classifications of Phragmites australis Using Object-Based Image Analysis. Remote Sens 15. https://doi.org/10.3390/rs15040989

Ao L, Feng K, Sheng K, Zhao H, He X, Chen Z (2023) TPENAS: A Two-Phase Evolutionary Neural Architecture Search for Remote Sensing Image Classification. Remote Sens 15: 2212. https://doi.org/10.3390/rs15082212

Ara M, Berglund M, Fahlvik N, Johansson U, Nilsson U (2022) Pre-Commercial Thinning Increases the Profitability of Norway Spruce Monoculture and Supports Norway Spruce–Birch Mixture over Full Rotations. For 2022, Vol 13, Page 1156 13: 1156. https://doi.org/10.3390/F13081156

Axelsson A, Lindberg E, Olsson H (2018) Exploring multispectral ALS data for tree species classification. Remote Sens 10. https://doi.org/10.3390/rs10020183

Axelsson P (2000) DEM generation from laser scanner data using adaptive tin models. Int Arch Photogramm Remote Sens 33: 110–117

Bachman CG (1979) Laser Radar Systems and Techniques. Artech House

Ball WJ, Kolabinski VS (1979) An Aerial Reconnaissance Of Softwood Regeneration On Mixedwood Sites in Saskatchewan, https://d1ied5g1xfgpx8.cloudfront.net/pdfs/11577.pdf

Bartels SF, Chen HYH, Wulder MA, White JC (2016) Trends in post-disturbance recovery rates of Canada’s forests following wildfire and harvest. For Ecol Manage 361: 194–207. https://doi.org/10.1016/J.FORECO.2015.11.015

Beland M, Parker G, Sparrow B, Harding D, Chasmer L, Phinn S, Antonarakis A, Strahler A (2019) On promoting the use of lidar systems in forest ecosystem research. For Ecol Manage 450: 117484. https://doi.org/10.1016/J.FORECO.2019.117484

Belgiu M, Drăgu L (2016) Random forest in remote sensing: A review of applications and future directions. ISPRS J Photogramm Remote Sens 114: 24–31. https://doi.org/10.1016/J.ISPRSJPRS.2016.01.011

Berglund E (2021) The Swedish model of forestry - Swedish Forest Industries Federation. Swedish For. Ind. https://www.forestindustries.se/bioeconomylife/how-we-manage-the-forest/the-swedish-model-of-forestry/. Accessed 15 October 2023

Bernard C, Mills JP, Talaya J, Remondino F (2019) Investigation into the potential of single photon airborne laser scanning technology. Int Arch Photogramm Remote Sens Spat Inf Sci - ISPRS Arch 42: 927–934. https://doi.org/10.5194/isprs-archives-XLII-2-W13-927-2019

Berrar D (2019) Cross-Validation. Encycl Bioinforma Comput Biol ABC Bioinforma 1–3: 542–545. https://doi.org/10.1016/B978-0-12-809633-8.20349-X

Bohlin J, Wallerman J, Fransson JES (2016) Deciduous forest mapping using change detection of multi-temporal canopy height models from aerial images acquired at leaf-on and leaf-off conditions. Scand J For Res 31: 517–525. https://doi.org/10.1080/02827581.2015.1130850

Bohlin J, Bohlin I, Jonzén J, Nilsson M (2017) Mapping forest attributes using data from stereophotogrammetry of aerial images and field data from the national forest inventory. Silva Fenn 51: 1–18. https://doi.org/10.14214/sf.2021

Breidenbach J, Næsset E, Gobakken T (2012) Improving k-nearest neighbor predictions in forest inventories by combining high and low density airborne laser scanning data. Remote Sens Environ 117: 358–365. https://doi.org/10.1016/j.rse.2011.10.010

Breiman L (2001) Random forests. Mach Learn 45: 5–32. https://doi.org/10.1023/A:1010933404324

Budei BC, St-Onge B, Hopkinson C, Audet FA (2018) Identifying the genus or species of individual trees using a three-wavelength airborne lidar system. Remote Sens Environ 204: 632–647. https://doi.org/10.1016/J.RSE.2017.09.037

Carr JC, Slyder JB (2018) Individual tree segmentation from a leaf-off photogrammetric

point cloud. Int J Remote Sens 39: 5195–5210. https://doi.org/10.1080/01431161.2018.1434330
Chadwick AJ, Goodbody TRH, Coops NC, Hervieux A, Bater CW, Martens LA, White B, Röeser D (2020) Automatic delineation and height measurement of regenerating conifer crowns under leaf-off conditions using uav imagery. Remote Sens 12: 1–26. https://doi.org/10.3390/RS12244104
Chen C, Jing L, Li H, Tang Y (2021) A new individual tree species classification method based on the resu-net model. Forests 12. https://doi.org/10.3390/F12091202
CSC – IT Center for Science Finland, 2022. Supercomputer Puhti Is Now Available for Researchers - Supercomputer Puhti Is Now Available for Researchers. CSC Company Site. h ttps://www.csc.fi/en/-/supertietokone-puhti-on-avattu-tutkijoiden-kayttoon.
Cutler DR, Edwards TC, Beard KH, Cutler A, Hess KT, Gibson J, Lawler JJ (2007) RANDOM FORESTS FOR CLASSIFICATION IN ECOLOGY. Ecology 88: 2783–2792. https://doi.org/10.1890/07-0539.1
Dalponte M, Ørka HO, Gobakken T, Gianelle D, Næsset E (2013) Tree species classification in boreal forests with hyperspectral data. IEEE Trans Geosci Remote Sens 51: 2632–2645. https://doi.org/10.1109/TGRS.2012.2216272
De Lombaerde E, Baeten L, Verheyen K, Perring MP, Ma S, Landuyt D (2021) Understorey removal effects on tree regeneration in temperate forests: A meta-analysis. J Appl Ecol 58: 9–20. https://doi.org/10.1111/1365-2664.13792
Degnan JJ (2016) Scanning, multibeam, single photon lidars for rapid, large scale, high resolution, topographic and bathymetric mapping. Remote Sens 8. https://doi.org/10.3390/rs8110958
Dumas N, Dupouey JL, Gégout JC, Boulanger V, Bontemps JD, Morneau F, Dalmasso M, Collet C (2022) Identification and spatial extent of understory plant species requiring vegetation control to ensure tree regeneration in French forests. Ann For Sci 79. https://doi.org/10.1186/S13595-022-01160-W
Eerikäinen K (2009) A Multivariate Linear Mixed-Effects Model for the Generalization of ... For Sci 55: 480–493. https://doi.org/https://doi.org/10.1093/forestscience/55.6.480
Eid T, Gobakken T, Næsset E (2004) Comparing stand inventories for large areas based on photo-interpretation and laser scanning by means of cost-plus-loss analyses. Scand J For Res 19: 512–523. https://doi.org/10.1080/02827580410019463
Fassnacht FE, Neumann C, Forster M, Buddenbaum H, Ghosh A, Clasen A, Joshi PK, Koch B (2014) Comparison of feature reduction algorithms for classifying tree species with hyperspectral data on three central european test sites. IEEE J Sel Top Appl Earth Obs Remote Sens 7: 2547–2561. https://doi.org/10.1109/JSTARS.2014.2329390
Fassnacht FE, Mangold D, Schäfer J, Immitzer M, Kattenborn T, Koch B, Latifi H (2017) Estimating stand density, biomass and tree species from very high resolution stereo-imagery-towards an all-in-one sensor for forestry applications? Forestry 90: 613–631. https://doi.org/10.1093/forestry/cpx014
Fassnacht FE, White JC, Wulder MA, Naesset E (2024) Remote sensing in forestry: current challenges, considerations and directions. For An Int J For Res 97: 11–37. https://doi.org/10.1093/FORESTRY/CPAD024
Fawagreh K, Gaber MM, Elyan E (2014) Random forests: from early developments to recent advancements. Syst Sci Control Eng An Open Access J 2: 602–609. https://doi.org/10.1080/21642583.2014.956265
Feduck C, McDermid GJ, Castilla G (2018) Detection of coniferous seedlings in UAV imagery. Forests 9. https://doi.org/10.3390/F9070432
Fraser BT, Congalton RG (2021) Monitoring Fine-Scale Forest Health Using Unmanned Aerial Systems (UAS) Multispectral Models. Remote Sens 2021, Vol 13, Page 4873 13:

4873. https://doi.org/10.3390/RS13234873
Fricker GA, Ventura JD, Wolf JA, North MP, Davis FW, Franklin J (2019) A convolutional neural network classifier identifies tree species in mixed-conifer forest from hyperspectral imagery. Remote Sens 11. https://doi.org/10.3390/rs11192326
Fromm M, Schubert M, Castilla G, Linke J, McDermid G (2019) Automated detection of conifer seedlings in drone imagery using convolutional neural networks. Remote Sens 11. https://doi.org/10.3390/rs11212585
Gallardo-Salazar JL, Pompa-García M (2020) Detecting individual tree attributes and multispectral indices using unmanned aerial vehicles: Applications in a pine clonal orchard. Remote Sens 12: 1–22. https://doi.org/10.3390/rs12244144
Gao Q, Lim S, Jia X (2018) Hyperspectral image classification using convolutional neural networks and multiple feature learning. Remote Sens 10. https://doi.org/10.3390/rs10020299
Gatziolis D, Fried JS, Monleon VS (2010) Challenges to estimating tree height via LiDAR in closed-canopy forest: a parable from western Oregon. For Sci 56(2) 139-155 139–155
Gislason PO, Benediktsson JA, Sveinsson JR (2006) Random Forests for land cover classification. Pattern Recognit Lett 27: 294–300. https://doi.org/10.1016/J.PATREC.2005.08.011
Goodbody TRH, Coops NC, Hermosilla T, Tompalski P, Crawford P (2018) Assessing the status of forest regeneration using digital aerial photogrammetry and unmanned aerial systems. Int J Remote Sens 39: 5246–5264. https://doi.org/10.1080/01431161.2017.1402387
Goodbody TRH, Coops NC, White JC (2019) Digital Aerial Photogrammetry for Updating Area-Based Forest Inventories: A Review of Opportunities, Challenges, and Future Directions. Curr For Reports 55–75. https://doi.org/10.1007/s40725-019-00087-2
Gorgens EB, Valbuena R, Rodriguez LCE (2017) A method for optimizing height threshold when computing airborne laser scanning metrics. Photogramm Eng Remote Sensing 83: 343–350. https://doi.org/10.14358/PERS.83.5.343
Guimarães N, Pádua L, Marques P, Silva N, Peres E, Sousa JJ (2020) Forestry Remote Sensing from Unmanned Aerial Vehicles: A Review Focusing on the Data, Processing and Potentialities. Remote Sens 2020, Vol 12, Page 1046 12: 1046. https://doi.org/10.3390/RS12061046
Guo X, Li H, Jing L, Wang P (2022) Individual Tree Species Classification Based on Convolutional Neural Networks and Multitemporal High-Resolution Remote Sensing Images. Sensors 22. https://doi.org/10.3390/S22093157
Häme T (1984) Interpretation Of Deciduous Trees And Shrubs In Conifer Seedling Stands From Landsat Imagery. Photogramm J Finl 9: 209–217
Haagsma M, Page GFM, Johnson JS, Still C, Waring KM, Sniezko RA, Selker JS (2020) Using Hyperspectral Imagery to Detect an Invasive Fungal Pathogen and Symptom Severity in Pinus strobiformis Seedlings of Different Genotypes. Remote Sens 2020, Vol 12, Page 4041 12: 4041. https://doi.org/10.3390/RS12244041
Haddow KA, King DJ, Pouliot DA, Pitt DG, Bell FW (2000) Early regeneration conifer identification and competition cover assessment using airborne digital camera imagery. For Chron 76: 915–928. https://doi.org/10.5558/tfc76915-6
Hall RJ, Aldred AH (1992) Forest regeneration appraisal with large-scale aerial photographs. For Chron 68: 142–150. https://doi.org/10.5558/TFC68142-1
Hartley RJL, Leonardo EM, Massam P, Watt MS, Estarija HJ, Wright L, Melia N, Pearse GD (2020) An assessment of high-density UAV point clouds for the measurement of

young forestry trials. Remote Sens 12: 1–20. https://doi.org/10.3390/rs12244039
Hartling S, Sagan V, Sidike P, Maimaitijiang M, Carron J (2019) Urban tree species classification using a worldview-2/3 and liDAR data fusion approach and deep learning. Sensors (Switzerland) 19: 1–23. https://doi.org/10.3390/s19061284
Haugerud RA, Harding DJ, Johnson SY, Harless JL, Weaver CS, Sherrod BL (2003) High-resolution lidar topography of the Puget Lowland, Washington - A bonanza for earth science. GSA Today 13: 4–10. https://doi.org/10.1130/1052-5173(2003)13
Honkavaara E, Khoramshahi E (2018) Radiometric correction of close-range spectral image blocks captured using an unmanned aerial vehicle with a radiometric block adjustment. Remote Sens 10. https://doi.org/10.3390/RS10020256
Honkavaara E, Saari H, Kaivosoja J, Pölönen I, Hakala T, Litkey P, Mäkynen J, Pesonen L (2013) Processing and assessment of spectrometric, stereoscopic imagery collected using a lightweight UAV spectral camera for precision agriculture. Remote Sens 5: 5006–5039. https://doi.org/10.3390/rs5105006
Huo L, Persson HJ, Lindberg E (2021) Early detection of forest stress from European spruce bark beetle attack, and a new vegetation index: Normalized distance red & SWIR (NDRS). Remote Sens Environ 255: 112240. https://doi.org/10.1016/J.RSE.2020.112240
Huuskonen S, Hynynen J (2006) Timing and intensity of precommercial thinning and their effects on the first commercial thinning in Scots pine stands. Silva Fenn 40: 645–662. https://doi.org/10.14214/SF.320
Huuskonen S, Haikarainen S, Sauvula-Seppälä T, Salminen H, Lehtonen M, Siipilehto J, Ahtikoski A, Korhonen KT, Hynynen J (2020) Benefits of juvenile stand management in Finland—impacts on wood production based on scenario analysis. For An Int J For Res 93: 458–470. https://doi.org/10.1093/forestry/cpz075
Hynynen J, Niemistö P, Viherä-Aarnio A, Brunner A, Hein S, Velling P (2010) Silviculture of birch (Betula pendula Roth and Betula pubescens Ehrh.) in Northern Europe. Forestry 83: 103–119. https://doi.org/10.1093/FORESTRY/CPP035
Hyyppä E, Yu X, Kaartinen H, Hakala T, Kukko A, Vastaranta M, Hyyppä J (2020) Comparison of Backpack, Handheld, Under-Canopy UAV, and Above-Canopy UAV Laser Scanning for Field Reference Data Collection in Boreal Forests. Remote Sens 2020, Vol 12, Page 3327 12: 3327. https://doi.org/10.3390/RS12203327
Hyyppä J, Inkinen M (1999) Detecting and estimating attribute for single trees using laser scanner. photogrametric J Finl 16: 27–42. https://doi.org/https://foto.aalto.fi/seura/julkaisut/pjf/pjf_e/1999/PJF1999_Hyyppa_and_Inkinen.pdf
Hyyppä J, Hyyppä H, Leckie D, Gougeon F, Yu X, Maltamo M (2008) Review of methods of small-footprint airborne laser scanning for extracting forest inventory data in boreal forests. Int J Remote Sens 29: 1339–1366. https://doi.org/10.1080/01431160701736489
Hyyppä J, Yu X, Hyyppä H, Vastaranta M, Holopainen M, Kukko A, Kaartinen H, Jaakkola A, Vaaja M, Koskinen J, Alho P (2012) Advances in forest inventory using airborne laser scanning. Remote Sens 4: 1190–1207. https://doi.org/10.3390/rs4051190
Immitzer M, Atzberger C, Koukal T (2012) Tree Species Classification with Random Forest Using Very High Spatial Resolution 8-Band WorldView-2 Satellite Data. Remote Sens 2012, Vol 4, Pages 2661-2693 4: 2661–2693. https://doi.org/10.3390/RS4092661
Järnstedt J, Pekkarinen A, Tuominen S, Ginzler C, Holopainen M, Viitala R (2012) Forest variable estimation using a high-resolution digital surface model. ISPRS J Photogramm Remote Sens 74: 78–84. https://doi.org/10.1016/J.ISPRSJPRS.2012.08.006
Jayathunga S, Pearse GD, Watt MS (2023) Unsupervised Methodology for Large-Scale Tree Seedling Mapping in Diverse Forestry Settings Using UAV-Based RGB Imagery. Remote Sens 2023, Vol 15, Page 5276 15: 5276. https://doi.org/10.3390/RS15225276

Junttila S, Näsi R, Koivumäki N, Imangholiloo M, Saarinen N, Raisio J, Holopainen M, Hyyppä H, Hyyppä J, Lyytikäinen-Saarenmaa P, Vastaranta M, Honkavaara E (2022) Multispectral Imagery Provides Benefits for Mapping Spruce Tree Decline Due to Bark Beetle Infestation When Acquired Late in the Season. Remote Sens 2022, Vol 14, Page 909 14: 909. https://doi.org/10.3390/RS14040909

Kaila S, Kiljunen N, Miettinen A, Valkonen S (2006) Effect of timing of precommercial thinning on the consumption of working time in Picea abies stands in Finland. Scand J For Res 21: 496–504. https://doi.org/10.1080/02827580601073263

Kanerva H, Honkavaara E, Näsi R, Hakala T, Junttila S, Karila K, Koivumäki N, Alves Oliveira R, Pelto-Arvo M, Pölönen I, Tuviala J, Östersund M, Lyytikäinen-Saarenmaa P (2022) Estimating Tree Health Decline Caused by Ips typographus L. from UAS RGB Images Using a Deep One-Stage Object Detection Neural Network. Remote Sens 2022, Vol 14, Page 6257 14: 6257. https://doi.org/10.3390/RS14246257

Kaplan A, Haenlein M (2019) Siri, Siri, in my hand: Who's the fairest in the land? On the interpretations, illustrations, and implications of artificial intelligence. Bus Horiz 62: 15–25. https://doi.org/10.1016/J.BUSHOR.2018.08.004

Kattenborn T, Leitloff J, Schiefer F, Hinz S (2021) Review on Convolutional Neural Networks (CNN) in vegetation remote sensing. ISPRS J Photogramm Remote Sens 173: 24–49. https://doi.org/10.1016/J.ISPRSJPRS.2020.12.010

Kee E, Chong JJ, Choong ZJ, Lau M (2023) A Comparative Analysis of Cross-Validation Techniques for a Smart and Lean Pick-and-Place Solution with Deep Learning. Electron 2023, Vol 12, Page 2371 12: 2371. https://doi.org/10.3390/ELECTRONICS12112371

Kelley J, Trofymow JAT, Bone C (2022) Combining Area-Based and Individual Tree Metrics for Improving Merchantable and Non-Merchantable Wood Volume Estimates in Coastal Douglas-Fir Forests. Remote Sens 14: 2204. https://doi.org/10.3390/rs14092204

Kellomäki S, Väisänen H, Kirschbaum MUF, Kirsikka-Aho S, Peltola H (2021) Effects of different management options of Norway spruce on radiative forcing through changes in carbon stocks and albedo. For An Int J For Res 94: 588–597. https://doi.org/10.1093/FORESTRY/CPAB010

Kellomäki S, Strandman H, Kirsikka-Aho S, Kirschbaum MUF, Peltola H (2023) Effects of thinning intensity and rotation length on albedo- and carbon stock-based radiative forcing in boreal Norway spruce stands. For An Int J For Res 96: 518–529. https://doi.org/10.1093/FORESTRY/CPAC058

Kim P (2017) Convolutional Neural Network. In: MATLAB Deep Learning. Apress, Berkeley, CA, pp 121–147

Kim S, Mcgaughey RJ, Andersen H, Schreuder G (2009) Tree species differentiation using intensity data derived from leaf-on and leaf-off airborne laser scanner data. Remote Sens Environ 113: 1575–1586. https://doi.org/10.1016/j.rse.2009.03.017

Kirby CL (1980) A camera and interpretation system for assessment of forest regeneration. Environ. Can., Can. For. Serv., North. For. Res. Cent. Edmonton, Alberta

Knapp N, Huth A, Fischer R (2021) Tree crowns cause border effects in area-based biomass estimations from remote sensing. Remote Sens 13. https://doi.org/10.3390/rs13081592

Korhonen K, Ahola A, Heikkinen J, Henttonen H, Hotanen J-P, Ihalainen A, Melin M, Pitkänen J, Räty M, Sirviö M, Strandström M (2021) Forests of Finland 2014–2018 and their development 1921–2018. Silva Fenn 55: 1–49. https://doi.org/10.14214/sf.10662

Kornilov A, Safonov I, Yakimchuk I (2022) A Review of Watershed Implementations for Segmentation of Volumetric Images. J Imaging 2022, Vol 8, Page 127 8: 127. https://doi.org/10.3390/JIMAGING8050127

Korpela I, Tuomola T, Tokola T, Dahlin B (2008) Appraisal of seedling stand vegetation with airborne imagery and discrete-return LiDAR - an exploratory analysis. Silva Fenn 42: 753–772. https://doi.org/10.14214/sf

Korpela I, Hovi A, Morsdorf F (2012) Understory trees in airborne LiDAR data - Selective mapping due to transmission losses and echo-triggering mechanisms. Remote Sens Environ 119: 92–104. https://doi.org/10.1016/j.rse.2011.12.011

Kotivuori E, Maltamo M, Korhonen L, Strunk JL, Packalen P (2021) Prediction error aggregation behaviour for remote sensing augmented forest inventory approaches. Forestry 94: 576–587. https://doi.org/10.1093/FORESTRY/CPAB007

Kuuluvainen T, Gauthier S (2018) Young and old forest in the boreal: critical stages of ecosystem dynamics and management under global change. For Ecosyst 5. https://doi.org/10.1186/S40663-018-0142-2

Lefsky MA, Cohen WB, Acker SA, Parker GG, Spies TA, Harding D (1999) Lidar Remote Sensing of the Canopy Structure and Biophysical Properties of Douglas-Fir Western Hemlock Forests. Remote Sens Environ 70: 339–361. https://doi.org/10.1016/S0034-4257(99)00052-8

Lefsky MA, Cohen WB, Parker GG, Harding DJ (2002) Lidar remote sensing for ecosystem studies. Bioscience 52: 19–30. https://doi.org/10.1641/0006-3568(2002)052[0019:LRSFES]2.0.CO;2

Leica (2021) Leica SPL100 Highest efficiency over large areas. Leica Geosystems. https://leica-geosystems.com/-/media/files/leicageosystems/products/datasheets/leica_spl100_ds.ashx?la=en&hash=A58C4573F50AD31E275025DC4DA7A8E6

Leica HxMap (2022) Leica HxMap

Li H, Hu B, Li Q, Jing L (2021) Cnn-based individual tree species classification using high-resolution satellite imagery and airborne lidar data. Forests 12: 1–22. https://doi.org/10.3390/f12121697

Li Y, Zhang H, Shen Q (2017) Spectral-spatial classification of hyperspectral imagery with 3D convolutional neural network. Remote Sens 9. https://doi.org/10.3390/rs9010067

Litjens G, Kooi T, Bejnordi BE, Setio AAA, Ciompi F, Ghafoorian M, van der Laak JAWM, van Ginneken B, Sánchez CI (2017) A survey on deep learning in medical image analysis. Med Image Anal 42: 60–88. https://doi.org/10.1016/j.media.2017.07.005

Liu Y;, Zhang H;, Cui Z;, Lei K;, Zuo Y;, Wang J;, Hu X;, Qiu H, Liu Y, Zhang H, Cui Z, Lei K, Zuo Y, Wang J, Hu X, Qiu H (2023) Very High Resolution Images and Superpixel-Enhanced Deep Neural Forest Promote Urban Tree Canopy Detection. Remote Sens 2023, Vol 15, Page 519 15: 519. https://doi.org/10.3390/RS15020519

Lopatin E, Poikonen P (2023) Cost-Effective Aerial Inventory of Spruce Seedlings Using Consumer Drones and Deep Learning Techniques with Two-Stage UAV Flight Patterns. For 2023, Vol 14, Page 973 14: 973. https://doi.org/10.3390/F14050973

Ma L, Liu Y, Zhang X, Ye Y, Yin G, Johnson BA (2019) Deep learning in remote sensing applications: A meta-analysis and review. ISPRS J Photogramm Remote Sens 152: 166–177. https://doi.org/10.1016/j.isprsjprs.2019.04.015

Ma M, Liu J, Liu M, Zeng J, Li Y (2021) Tree Species Classification Based on Sentinel-2 Imagery and Random Forest Classifier in the Eastern Regions of the Qilian Mountains. For 2021, Vol 12, Page 1736 12: 1736. https://doi.org/10.3390/F12121736

Maltamo M, Packalen P, Kangas A (2021) From comprehensive field inventories to remotely sensed wall-to-wall stand attribute data — a brief history of management inventories in the Nordic countries. Can J For Res 51: 257–266. https://doi.org/10.1139/cjfr-2020-0322

Martins GB, La Rosa LEC, Happ PN, Filho LCTC, Santos CJF, Feitosa RQ, Ferreira MP (2021) Deep learning-based tree species mapping in a highly diverse tropical urban

setting. Urban For Urban Green 64. https://doi.org/10.1016/j.ufug.2021.127241
Mäyrä J, Keski-Saari S, Kivinen S, Tanhuanpää T, Hurskainen P, Kullberg P, Poikolainen L, Viinikka A, Tuominen S, Kumpula T, Vihervaara P (2021) Tree species classification from airborne hyperspectral and LiDAR data using 3D convolutional neural networks. Remote Sens Environ 256. https://doi.org/10.1016/j.rse.2021.112322
Melin M, Matala J, Mehtätalo L, Suvanto A, Packalen P (2015) Detecting moose (Alces alces) browsing damage in young boreal forests from airborne laser scanning data. Can J For Res 46: 10–19. https://doi.org/10.1139/CJFR-2015-0326
MetsäGroup (2020) Facts about Nordic forests – what you should know about Nordic forests and forestry. MetsäGroup 21
Mielcarek M, Kamińska A, Stereńczak K (2020) Digital Aerial Photogrammetry (DAP) and Airborne Laser Scanning (ALS) as Sources of Information about Tree Height: Comparisons of the Accuracy of Remote Sensing Methods for Tree Height Estimation. Remote Sens 2020, Vol 12, Page 1808 12: 1808. https://doi.org/10.3390/RS12111808
Mielikäinen K, Hynynen J (2003) Silvicultural management in maintaining biodiversity and resistance of forests in Europe–boreal zone: case Finland. J Environ Manage 67: 47–54. https://doi.org/10.1016/S0301-4797(02)00187-1
Minařík R, Langhammer J, Lendzioch T, Alvarez Taboada F, Govedarica M (2021) Detection of Bark Beetle Disturbance at Tree Level Using UAS Multispectral Imagery and Deep Learning. Remote Sens 2021, Vol 13, Page 4768 13: 4768. https://doi.org/10.3390/RS13234768
Mitri GH, Gitas IZ (2013) Mapping post-fire forest regeneration and vegetation recovery using a combination of very high spatial resolution and hyperspectral satellite imagery. Int J Appl Earth Obs Geoinf 20: 60–66. https://doi.org/10.1016/J.JAG.2011.09.001
Montaghi A, Corona P, Dalponte M, Gianelle D, Chirici G, Olsson H (2013) Airborne laser scanning of forest resources: An overview of research in Italy as a commentary case study. Int J Appl Earth Obs Geoinf 23: 288–300. https://doi.org/10.1016/J.JAG.2012.10.002
Næsset E (2002) Predicting forest stand characteristics with airborne scanning laser using a practical two-stage procedure and field data. 80: 88–99
Næsset E (2004) Practical large-scale forest stand inventory using a small-footprint airborne scanning laser. Scand J For Res 19: 164–179. https://doi.org/10.1080/02827580310019257
Næsset E (2005) Assessing sensor effects and effects of leaf-off and leaf-on canopy conditions on biophysical stand properties derived from small-footprint airborne laser data. Remote Sens Environ 98: 356–370. https://doi.org/10.1016/J.RSE.2005.07.012
Næsset E (2014) Area-Based Inventory in Norway – From Innovation to an Operational Reality. In: Forestry Applications of Airborne Laser Scanning. pp 215–240
Næsset E, Bjerknes K-O (2001) Estimating tree heights and number of stems in young forest stands using airborne laser scanner data. Remote Sens Environ 78: 328–340. https://doi.org/10.1016/S0034-4257(01)00228-0
Næsset E, Gobakken T, Holmgren J, Hyyppä H, Hyyppä J, Maltamo M, Nilsson M, Olsson H, Persson Å, Söderman U (2004) Laser scanning of forest resources: The nordic experience. Scand J For Res 19: 482–499. https://doi.org/10.1080/02827580410019553
Närhi M, Maltamo M, Packalén P, Peltola H, Soimasuo J (2008) Kuusen taimikoiden inventointi ja taimikonhoidon kiireellisyyden määrittäminen laserkeilauksen ja metsäsuunnitelmatietojen avulla. Metsätieteen Aikakausk 2008: 5–15. https://doi.org/10.14214/ma.6419

Näslund, M. 1936. Skogsförsöksanstaltens gallrings-försök i tallskog. Meddelanden från Statens Skogs-försöksanstalt 29. 169 p. (1936)

Natesan S, Armenakis C, Vepakomma U (2020) Individual tree species identification using dense convolutional network (Densenet) on multitemporal RGB images from UAV. J Unmanned Veh Syst 8: 310–333. https://doi.org/10.1139/juvs-2020-0014

Nelson R, Krabill W, Tonelli J (1988) Estimating forest biomass and volume using airborne laser data. Remote Sens Environ 24: 247–267. https://doi.org/10.1016/0034-4257(88)90028-4

Nevalainen O, Honkavaara E, Tuominen S, Viljanen N, Hakala T, Yu X, Hyyppä J, Saari H, Pölönen I, Imai NN, Tommaselli AMG (2017) Individual tree detection and classification with UAV-Based photogrammetric point clouds and hyperspectral imaging. Remote Sens 9. https://doi.org/10.3390/rs9030185

Nezami S, Khoramshahi E, Nevalainen O, Pölönen I, Honkavaara E (2020) Tree species classification of drone hyperspectral and RGB imagery with deep learning convolutional neural networks. Remote Sens 12. https://doi.org/10.3390/rs12071070

Nilsson M, Nordkvist K, Jonzén J, Lindgren N, Axensten P, Wallerman J, Egberth M, Larsson S, Nilsson L, Eriksson J, Olsson H (2017) A nationwide forest attribute map of Sweden predicted using airborne laser scanning data and field data from the National Forest Inventory. Remote Sens Environ 194: 447–454. https://doi.org/10.1016/j.rse.2016.10.022

Nilsson U, Luoranen J, Kolström T, Örlander G, Puttonen P, Kolstro¨m T, Kolstro¨m K, Go¨go¨ran G, Rlander O¨ (2010) Reforestation with planting in northern Europe. Scand J For Res 25: 283–294. https://doi.org/10.1080/02827581.2010.498384

Økseter R, Bollandsås OM, Gobakken T, Næsset E (2015) Modeling and predicting aboveground biomass change in young forest using multi-temporal airborne laser scanner data. Scand J For Res 30: 458–469. https://doi.org/10.1080/02827581.2015.1024733

Onishi M, Ise T (2021) Explainable identification and mapping of trees using UAV RGB image and deep learning. Sci Reports 2021 111 11: 1–15. https://doi.org/10.1038/s41598-020-79653-9

Ørka HO, Gobakken T, Næsset E (2016) Predicting Attributes of Regeneration Forests Using Airborne Laser Scanning. Can J Remote Sens 42: 541–553. https://doi.org/10.1080/07038992.2016.1199269

Ørka HO, Næsset E, Bollandsås OM (2010) Effects of different sensors and leaf-on and leaf-off canopy conditions on echo distributions and individual tree properties derived from airborne laser scanning. Remote Sens Environ 114: 1445–1461. https://doi.org/10.1016/J.RSE.2010.01.024

Packalen P, Strunk JL, Pitkänen JA, Temesgen H, Maltamo M (2015) Edge-Tree Correction for Predicting Forest Inventory Attributes Using Area-Based Approach With Airborne Laser Scanning. IEEE J Sel Top Appl Earth Obs Remote Sens 8: 1274–1280. https://doi.org/10.1109/JSTARS.2015.2402693

Packalén P, Maltamo M (2007) The k-MSN method for the prediction of species-specific stand attributes using airborne laser scanning and aerial photographs. Remote Sens Environ 109: 328–341. https://doi.org/10.1016/J.RSE.2007.01.005

Parkan MJ (2019) Combined use of airborne laser scanning and hyperspectral imaging for forest inventories. https://doi.org/10.5075/epfl-thesis-9033

Parkitna K, Krok G, Miścicki S, Ukalski K, Lisańczuk M, Mitelsztedt K, Magnussen S, Markiewicz A, Stereńczak K (2021) Modelling growing stock volume of forest stands with various ALS area-based approaches. For An Int J For Res 1–21. https://doi.org/10.1093/forestry/cpab011

Pascual A (2019) Using tree detection based on airborne laser scanning to improve forest inventory considering edge effects and the co-registration factor. Remote Sens 11. https://doi.org/10.3390/rs11222675

Pearse GD, Tan AYS, Watt MS, Franz MO, Dash JP (2020) Detecting and mapping tree seedlings in UAV imagery using convolutional neural networks and field-verified data. ISPRS J Photogramm Remote Sens 168: 156–169. https://doi.org/10.1016/j.isprsjprs.2020.08.005

Pedregosa F, Varoquaux G ̈el, Gramfort A, Michel V, Thirion B, Grisel O, Blondel M, Prettenhofer P, Weiss R, Dubourg V, Vanderplas J, Passos A, Cournapeau D, Brucher M, Perrot M, Duchesnay E (2011) Scikit-learn: Machine Learning in Python. J Mach Learn Res 12: 2825–2830

Pleşoianu AI, Stupariu MS, Şandric I, Pătru-Stupariu I, Drăguţ L (2020) Individual tree-crown detection and species classification in very high-resolution remote sensing imagery using a deep learning ensemble model. Remote Sens 12. https://doi.org/10.3390/RS12152426

Pouliot DA, King DJ, Pitt DG (2005) Development and evaluation of an automated tree detection-delineation algorithm for monitoring regenerating coniferous forests. Can J For Res 35: 2332–2345. https://doi.org/10.1139/x05-145

Pouliot DA, King DJ, Pitt DG (2006) Automated assessment of hardwood and shrub competition in regenerating forests using leaf-off airborne imagery. Remote Sens Environ 102: 223–236. https://doi.org/10.1016/j.rse.2006.02.008

Prasad MPS, Senthilrajan A (2022) A Novel CNN-KNN based Hybrid Method for Plant Classification. J Algebr Stat 13: 498–502

Puliti S, Ene LT, Gobakken T, Næsset E (2017) Use of partial-coverage UAV data in sampling for large scale forest inventories. Remote Sens Environ 194: 115–126. https://doi.org/10.1016/J.RSE.2017.03.019

Puliti S, Solberg S, Granhus A (2019) Use of UAV photogrammetric data for estimation of biophysical properties in forest stands under regeneration. Remote Sens 11. https://doi.org/10.3390/RS11030233

Puliti S, Dash JP, Watt MS, Breidenbach J, Pearse GD (2020) A comparison of UAV laser scanning, photogrammetry and airborne laser scanning for precision inventory of small-forest properties. For An Int J For Res 93: 150–162. https://doi.org/10.1093/FORESTRY/CPZ057

Quan Y, Li M, Hao Y, Liu J, Wang B (2023) Tree species classification in a typical natural secondary forest using UAV-borne LiDAR and hyperspectral data. GIScience Remote Sens 60. https://doi.org/10.1080/15481603.2023.2171706

Räty J, Varvia P, Korhonen L, Savolainen P, Maltamo M, Packalen P (2022) A Comparison of Linear-Mode and Single-Photon Airborne LiDAR in Species-Specific Forest Inventories. IEEE Trans Geosci Remote Sens 60: 1–14. https://doi.org/10.1109/TGRS.2021.3060670

Raczko E, Zagajewski B (2017) Comparison of support vector machine, random forest and neural network classifiers for tree species classification on airborne hyperspectral APEX images. Eur J Remote Sens 50: 144–154. https://doi.org/10.1080/22797254.2017.1299557

Rana P, Mattila U, Mehtätalo L, Siipilehto J, Hou Z, Xu Q, Tokola T (2023) Monitoring seedling stands using national forest inventory and multispectral airborne laser scanning data. Can J For Res 53: 302–313. https://doi.org/10.1139/cjfr-2022-0135

Rantala S (2011) Finnish forestry: practice and management. Metsäkustannus Oy

Röder M, Latifi H, Hill S, Wild J, Svoboda M, Brůna J, Macek M, Nováková MH, Gülch E, Heurich M (2018) Application of optical unmanned aerial vehicle-based imagery for the inventory of natural regeneration and standing deadwood in post-disturbed spruce forests. Int J Remote Sens 00: 1–22. https://doi.org/10.1080/01431161.2018.1441568

Safonova A, Hamad Y, Alekhina A, Kaplun D (2022) Detection of Norway Spruce Trees (Picea Abies) Infested by Bark Beetle in UAV Images Using YOLOs Architectures. IEEE Access 10: 10384–10392. https://doi.org/10.1109/ACCESS.2022.3144433

Sewak M, Karim MR, Pujari P (2018) Practical Convolutional Neural Networks : Implement advanced deep learning models using Python. Packt Publishing

Shang X, Chisholm LA (2014) Classification of Australian native forest species using hyperspectral remote sensing and machine-learning classification algorithms. IEEE J Sel Top Appl Earth Obs Remote Sens 7: 2481–2489. https://doi.org/10.1109/JSTARS.2013.2282166

Shinzato ET, Shimabukuro YE, Coops NC, Tompalski P, Gasparoto EA (2017) Integrating area-based and individual tree detection approaches for estimating tree volume in plantation inventory using aerial image and airborne laser scanning data. IForest 10: 296–302. https://doi.org/10.3832/IFOR1880-009

Smith JL, Campbell CD, Mead RA (1986) Imaging and Identifying Loblolly Pine Seedlings after the First Growing Season on 35MM Aerial Photography. Can J Remote Sens 12: 19–27. https://doi.org/10.1080/07038992.1986.10855093

Snavely N, Seitz SM, Szeliski R (2008) Modeling the world from Internet photo collections. Int J Comput Vis 80: 189–210. https://doi.org/10.1007/S11263-007-0107-3/METRICS

Solvin TM, Puliti S, Steffenrem A (2020) Use of UAV photogrammetric data in forest genetic trials: measuring tree height, growth, and phenology in Norway spruce (Picea abies L. Karst.). Scand J For Res 35: 322–333. https://doi.org/10.1080/02827581.2020.1806350

Sun Y, Xin Q, Huang J, Huang B, Zhang H (2019) Characterizing Tree Species of a Tropical Wetland in Southern China at the Individual Tree Level Based on Convolutional Neural Network. IEEE J Sel Top Appl Earth Obs Remote Sens 12: 4415–4425. https://doi.org/10.1109/JSTARS.2019.2950721

Swatantran A, Tang H, Barrett T, Decola P, Dubayah R (2016) Rapid, high-resolution forest structure and terrain mapping over large areas using single photon lidar. Sci Rep 6: 1–12. https://doi.org/10.1038/srep28277

Tapio. (2006). Hyvän metsänhoidon suositukset. [Recommendations for forest management in Finland]. Forest Development Centre Tapio. Metsäkustannus oy. 100 p. [In Finnish]

Thiel C, Schmullius C (2017) Comparison of UAV photograph-based and airborne lidar-based point clouds over forest from a forestry application perspective. Int J Remote Sens 38: 2411–2426. https://doi.org/10.1080/01431161.2016.1225181

Torresan C, Berton A, Carotenuto F, Di Gennaro SF, Gioli B, Matese A, Miglietta F, Vagnoli C, Zaldei A, Wallace L (2017) Forestry applications of UAVs in Europe: a review. Int J Remote Sens 38: 2427–2447. https://doi.org/10.1080/01431161.2016.1252477

Trier ØD, Salberg AB, Kermit M, Rudjord Ø, Gobakken T, Næsset E, Aarsten D (2018) Tree species classification in Norway from airborne hyperspectral and airborne laser scanning data. Eur J Remote Sens 51: 336–351. https://doi.org/10.1080/22797254.2018.1434424

Tuominen S, Balazs A, Saari H, Pölönen I, Sarkeala J, Viitala R (2015) Unmanned aerial system imagery and photogrammetric canopy height data in area-based estimation of forest variables. Silva Fenn 49. https://doi.org/10.14214/SF.1348

Turkulainen E, Honkavaara E, Näsi R, Oliveira RA, Hakala T, Junttila S, Karila K, Koivumäki N, Pelto-Arvo M, Tuviala J, Östersund M, Pölönen I, Lyytikäinen-Saarenmaa P (2023) Comparison of Deep Neural Networks in the Classification of Bark Beetle-Induced Spruce Damage Using UAS Images. Remote Sens 2023, Vol 15, Page 4928 15: 4928. https://doi.org/10.3390/RS15204928

Uotila K (2017) Optimization of early cleaning and precommercial thinning methods in juvenile stand management of Norway

Uotila K, Saksa T (2014) Effects of early cleaning on young Picea abies stands. Scand J For Res 29: 111–119. https://doi.org/10.1080/02827581.2013.869349

Vastaranta M, Holopainen M, Yu X, Hyyppä J, Mäkinen A, Rasinmäki J, Melkas T, Kaartinen H, Hyyppä H (2011) Effects of individual tree detection error sources on forest management planning calculations. Remote Sens 3: 1614–1626. https://doi.org/10.3390/rs3081614

Vastaranta M, Kankare V, Holopainen M, Yu X, Hyyppä J, Hyyppä H (2012) Combination of individual tree detection and area-based approach in imputation of forest variables using airborne laser data. ISPRS J Photogramm Remote Sens 67: 73–79. https://doi.org/10.1016/j.isprsjprs.2011.10.006

Vepakomma U, Cormier D, Thiffault N (2015) Potential of UAV based convergent photogrammetry in monitoring regeneration standards. Int Arch Photogramm Remote Sens Spat Inf Sci - ISPRS Arch 40: 281–285. https://doi.org/10.5194/isprsarchives-XL-1-W4-281-2015

Vepakomma U, Cormier D, Hansson L, Talbot B (2023) Remote Sensing at Local Scales for Operational Forestry. Adv Glob Chang Res 74: 657–682. https://doi.org/10.1007/978-3-031-15988-6_27/FIGURES/8

Villikka M, Packalén P, Maltamo M (2012) The suitability of leaf-off airborne laser scanning data in an area-based forest inventory of coniferous and deciduous trees. Silva Fenn 46: 99–110. https://doi.org/10.14214/sf.68

Wang H, Zhao Y, Pu R, Zhang Z (2015) Mapping Robinia Pseudoacacia Forest Health Conditions by Using Combined Spectral, Spatial, and Textural Information Extracted from IKONOS Imagery and Random Forest Classifier. Remote Sens 2015, Vol 7, Pages 9020-9044 7: 9020–9044. https://doi.org/10.3390/RS70709020

Wang Y, Hyyppa J, Liang X, Kaartinen H, Yu X, Lindberg E, Holmgren J, Qin Y, Mallet C, Ferraz A, Torabzadeh H, Morsdorf F, Zhu L, Liu J, Alho P (2016) International Benchmarking of the Individual Tree Detection Methods for Modeling 3-D Canopy Structure for Silviculture and Forest Ecology Using Airborne Laser Scanning. IEEE Trans Geosci Remote Sens 54: 5011–5027. https://doi.org/10.1109/TGRS.2016.2543225

Wang Y, Lehtomäki M, Liang X, Pyörälä J, Kukko A, Jaakkola A, Liu J, Feng Z, Chen R, Hyyppä J (2019) Is field-measured tree height as reliable as believed – A comparison study of tree height estimates from field measurement, airborne laser scanning and terrestrial laser scanning in a boreal forest. ISPRS J Photogramm Remote Sens 147: 132–145. https://doi.org/10.1016/j.isprsjprs.2018.11.008

Wehr A, Lohr U (1999) Airborne laser scanning—an introduction and overview. ISPRS J Photogramm Remote Sens 54: 68–82.https://doi.org/10.1016/S0924-2716(99)00011-8

White JC, Wulder M a, Varhola A, Vastaranta M, Coops NC, Cook BD, Pitt D, Woods M (2013a) A best practices guide for generating forest inventory attributes from airborne laser scanning data using an area-based approach

White JC, Wulder MA, Vastaranta M, Coops NC, Pitt D, Woods M (2013b) The utility of image-based point clouds for forest inventory: A comparison with airborne laser scanning. Forests 4: 518–536. https://doi.org/10.3390/f4030518

White JC, Arnett JTTR, Wulder MA, Tompalski P, Coops NC (2015) Evaluating the impact of leaf-on and leaf-off airborne laser scanning data on the estimation of forest inventory attributes with the area-based approach. Can J For Res 45: 1498–1513. https://doi.org/10.1139/cjfr-2015-0192

Wulder MA, White JC, Nelson RF, Næsset E, Ørka HO, Coops NC, Hilker T, Bater CW, Gobakken T (2012) Lidar sampling for large-area forest characterization: A review. Remote Sens Environ 121: 196–209. https://doi.org/10.1016/j.rse.2012.02.001

Wunderle AL, Franklin SE, Guo XG (2007) Regenerating boreal forest structure estimation using SPOT-5 pansharpened imagery. Int J Remote Sens 28: 4351–4364. https://doi.org/10.1080/01431160701244849

Xi Y, Ren C, Wang Z, Wei S, Bai J, Zhang B, Xiang H, Chen L (2019) Mapping tree species composition using OHS-1 hyperspectral data and deep learning algorithms in Changbai mountains, Northeast China. Forests 10. https://doi.org/10.3390/f10090818

Yaloveha V, Hlavcheva D, Podorozhniak A (2021) Spectral Indexes Evaluation for Satellite Images Classification using CNN. J Inf Organ Sci 45: 435–449. https://doi.org/10.31341/JIOS.45.2.5

Yan S, Jing L, Wang H (2021) A new individual tree species recognition method based on a convolutional neural network and high-spatial resolution remote sensing imagery. Remote Sens 13: 1–21. https://doi.org/10.3390/RS13030479

Ye N, Morgenroth J, Xu C, Chen N (2021) Indigenous forest classification in New Zealand – A comparison of classifiers and sensors. Int J Appl Earth Obs Geoinf 102: 102395. https://doi.org/10.1016/j.jag.2021.102395

Yu X, Hyyppä J, Litkey P, Kaartinen H, Vastaranta M, Holopainen M (2017) Single-Sensor Solution to Tree Species Classification Using Multispectral Airborne Laser Scanning. Remote Sens 9: 108. https://doi.org/10.3390/rs9020108

Yu X, Kukko A, Kaartinen H, Wang Y, Liang X, Matikainen L, Hyyppä J (2020) Comparing features of single and multi-photon lidar in boreal forests. ISPRS J Photogramm Remote Sens 168: 268–276. https://doi.org/10.1016/j.isprsjprs.2020.08.013

Zahawi RA, Dandois JP, Holl KD, Nadwodny D, Reid JL, Ellis EC (2015) Using lightweight unmanned aerial vehicles to monitor tropical forest recovery. Biol Conserv 186: 287–295. https://doi.org/10.1016/j.biocon.2015.03.031

Zhang B, Zhao L, Zhang X (2020) Three-dimensional convolutional neural network model for tree species classification using airborne hyperspectral images. Remote Sens Environ 247. https://doi.org/10.1016/J.RSE.2020.111938

Zhao H, Sun Y, Jia W, Wang F, Zhao Z, Wu S (2023) Study on the Regeneration Probability of Understory Coniferous Saplings in the Liangshui Nature Reserve Based on Four Modeling Techniques. Remote Sens 2023, Vol 15, Page 4869 15: 4869. https://doi.org/10.3390/RS15194869